CHAPTER ONE

Modeling Syndromic Congenital Heart Defects in Zebrafish

Meagan G. Grant[1], Victoria L. Patterson[1], Daniel T. Grimes, Rebecca D. Burdine[2]
Princeton University, Princeton, NJ, United States
[2]Corresponding author: e-mail address: rburdine@Princeton.EDU

Contents

Abstract

Cardiac development is a dynamic process regulated by spatial and temporal cues that are integrated to effect molecular, cellular, and tissue-level events that form the adult heart. Disruption of these highly orchestrated events can be devastating for cardiac form and function. Aberrations in heart development result in congenital heart defects (CHDs), which affect 1 in 100 infants in the United States each year. Zebrafish have

[1] These authors contributed equally.

Current Topics in Developmental Biology, Volume 124
ISSN 0070-2153
http://dx.doi.org/10.1016/bs.ctdb.2016.11.010

proven informative as a model organism to understand both heart development and the mechanisms associated with CHDs due to the similarities in heart morphogenesis among vertebrates, as well as their genetic tractability and amenability to live imaging. In this review, we discuss the mechanisms of zebrafish heart development and the utility of zebrafish for understanding syndromic CHDs, those cardiac abnormalities that occur in the context of multisystem disorders. We conclude with avenues of zebrafish research that will potentially inform future therapeutic approaches for the treatment of CHDs.

1. INTRODUCTION

1.1 Overview of Congenital Heart Defects

During human embryogenesis, the fetal heart undergoes a series of dynamic morphogenetic events. Cardiac progenitor cells (CPCs) are specified and differentiated based on location in order to migrate and form a primitive heart tube. Multiple signaling and patterning events occurring throughout this process ensure the heart is positioned appropriately and that the embryonic heart tube transforms into a contractile, multichambered organ capable of pumping blood throughout the body. The processes driving human heart development are myriad and complex. Disruption of these processes results in congenital heart defects (CHDs), the leading cause of infant mortality arising from structural birth defects in the United States. CHDs differ in prevalence, severity, and the heart tissues affected, existing in isolation or in the context of syndromic disorders affecting multiple organ systems, and can arise as a result of multigenic causes or mutations in single genes (Mozaffarian et al., 2016). Animal models are critical to studying these pathologies, with zebrafish emerging as a premier tool for understanding CHDs.

1.2 Zebrafish as a Model of Vertebrate Cardiogenesis and CHDs

The zebrafish is an excellent system for studying heart development and the aberrations in morphogenesis that result in cardiac defects. The human heart is comprised of two upper chambers (the left and right atria) and two lower chambers (the left and right ventricles). A septum separates the left atrium from the right atrium and the left ventricle from the right ventricle. Despite the fact that the zebrafish heart consists of a single atrium and ventricle that are not septated, the morphogenetic behaviors required for heart development in humans and zebrafish are strikingly similar. Moreover, many of the genes involved in heart development (Table 1) are conserved (for example, see Bruneau, 2008; Richards & Garg, 2010; Szeto et al., 2002), and are useful in visualizing specific cell types in the heart (Table 2). Other facets making zebrafish ideal for cardiovascular studies include their fecundity,

Table 1 Human and Zebrafish Cardiac Phenotypes Caused by Mutations in Single Genes Associated With Nonsyndromic Heart Defects

Gene	Patient CHD	Zebrafish Heart Defects	References
GATA4	ASD, VSD	Cardiomyopathy, defective cardiac looping, chamber expansion, blood circulation, and heart tube displacement	Bruneau (2008), Holtzinger and Evans (2005), and Richards and Garg (2010)
GATA6	AVSD, PTA, TOF	Cardia bifida, impaired cardiac looping, and heart tube fusion defects	Holtzman, Schoenebeck, Tsai, and Yelon (2007) and Kodo and Yamagishi (2010)
MYH6	ASD, HCM	Dilated atrium, weakened atrial contractility, defective myofibrillar organization, thickening of ventricular wall, and narrowing of ventricular lumen	Auman et al. (2007), Berdougo, Coleman, Lee, Stainier and Yelon (2003), Bruneau (2008), and Richards and Garg (2010)
NKX2.5	ASD, VSD, conduction defects, TOF, TGA, valve defects	Defective proliferation of SHF progenitors, misshapen atria, smaller ventricle, loss of SHF-derived ventricular myocardium and OFT smooth muscle	Bruneau (2008), Guner-Ataman et al. (2013), Richards and Garg (2010), and Targoff, Schell, and Yelon (2008)
TBX20	ASD, VSD	Abnormal contractility, no blood circulation, edema, abnormal cardiac looping and chamber morphology	Bruneau (2008) and Szeto, Griffin, and Kimelman (2002)
HAND2	TOF, PS, AVSD, VSD-DORV	Reduced myocardium, endocardium fails to form cone	Palencia-Desai et al. (2015), Shen et al. (2010), and Yelon et al. (2000)

ASD, atrial septal defect; *AVSD*, atrioventricular septal defect; *DCM*, dilated cardiomyopathy; *DORV*, double outlet right ventricle; *HCM*, hypertrophic cardiomyopathy; *PS*, pulmonary stenosis; *PTA*, persistent truncus arteriosus; *TGA*, transposition of the great arteries; *TOF*, tetralogy of fallot; *VSD*, ventricular septal defect.

Table 2 Markers for Cell Types in the Zebrafish Heart

Cell Type	Transgenic Marker	Gene Marker	Antibody or Fluorescent Indicator	Functional Assay	References
Myocardial	*Tg(myl7:GFP), Tg(cmlc2:dsred2-nuc)*	*myl7*[a], *vmhc, amhc*	MF20, S46	Cardiac conduction: *Tg(cmlc2:gCaMP)*^{s878}	Miura and Yelon (2011)
				Timing of differentiation: *Tg(cmlc2:Kaede)*	
Endocardial and endothelial	*Tg(flk1:EGFP), Tg(fli1:EGFP)*	*flk1 (kdrl/vegfr2), fli1*	Kdrl	Angioblast migration and vascular tube formation: *Tg(flk1:EGFP)*	Miura and Yelon (2011) and Poon, Liebling, Kondrychyn, Garcia-Lecea, and Korzh (2010)
Epicardial	*Tg(tcf21:DsRed2), Tg(wt1b:eGFP)*	*tcf21*	Raldh2 (also in endocardium)	Cellular contributions of the epicardium: *tcf21:CreER; gata5:RnG*	Kikuchi et al. (2011) and Perner, Englert, and Bollig (2007)
Second heart field	*Tg(ltbp3:TagRFP2Acre); Tg(cmlc2:CSY), Tg(nkx2.5::ZsYellow); Tg(cmlc2::CSY)*	*ltbp3*	Eln2 and DAF-2DA (BA), Isl1	Contributions to SHF-derived structures: photoconversion of *Tg(nkx2.5:Kaede)* transgenics	de Pater et al. (2009), Grimes, Stadt, Shepherd, and Kirby (2006), Guner-Ataman et al. (2013), and Zhou et al. (2011)
	BA smooth muscle cells: Tg(eln2:CSY)			Cellular contributions to OFT SMCs: *Tg(eln2:CSY)* reporter strain crossed with a driver strain [*Tg(ltbp3::TagRFP2Acre), Tg(gata4:ERCreER), or Tg(nkx2.5:ERCreER)*, for example]	

Erythrocyte	*Tg(Gata1:DsRed), Tg(Gata1:EGFP)*	*gata1*	–	Blood flow through vessels: *Tg(Gata1:Dsred); Tg(Fli1:EGFP)*	De Domenico et al. (2007), Miura and Yelon (2011), and Poon et al. (2010)
				Hemoglobin production: o-dianisidine staining	
				Tissue iron delivery: Prussian blue staining	

[a]*myl7* was formerly referred to as *cmlc2*.

external fertilization, rapid development, and transparency. These qualities allow in vivo time-lapse imaging, and examination of multiple stages and aspects of heart development. Additionally, the small size of zebrafish embryos allows for passive diffusion of oxygen, permitting survival of the organism for several days despite cardiovascular defects (Stainier, 2001). Thus, mutants with abrogated cardiovascular function can be studied for longer than is possible in mammalian organisms where cardiac defects cause early lethality. Indeed, many zebrafish cardiovascular mutants, some discovered decades ago (Haffter et al., 1996; Stainier et al., 1996; Stainier, Weinstein, Detrich, Zon, & Fishman, 1995), have provided important insights into the molecular and cellular processes underlying vertebrate heart formation. Finally, methodologies for manipulating the genome in order to generate tools and disease models are rapidly advancing in zebrafish. These aspects make zebrafish a versatile model for furthering our understanding of human CHDs. Here we discuss how this system has been successfully used to understand the genetic basis of heart development and to identify the mechanisms of syndromic heart defects in humans (Table 3).

Table 3 Syndromic Heart Defects: Causative Genes, Human Heart Defects, and Zebrafish Phenotypes

Syndrome	Example Genes Involved	Patient CHDs Include	Zebrafish Phenotypes
Ciliopathies and Heterotaxy	*PKD2, PKD1L1*	Dextrocardia	Aberrant heart looping laterality
RASopathies	*PTPN11, RIT1, NF1, RAF1, KRAS, HRAS*	HCM, CoA, ASD, VSD, PVS, PS	Impaired cardiac jogging and looping, reduced cardiac function, edema, defects in heart size, hypoplastic chambers, valve defects, thickening of heart walls, delays in heart morphogenesis
Cohesinopathies	*NIPBL, RAD21*	VSD, ASD, PS, TOF, HLHS	Reduced heart size, impaired cardiac looping, valve defects
CHARGE	*CHD7, SEMA3A, SEMA3E*	TOF,PDA, DORV, VSD, ASD, AVSD, LVOTO, RVOTO	Dysmorphic chambers, edema, reduced blood flow, weak heartbeat, abnormal narrowing of dorsal aorta

Table 3 Syndromic Heart Defects: Causative Genes, Human Heart Defects, and Zebrafish Phenotypes—cont'd

Syndrome	Example Genes Involved	Patient CHDs Include	Zebrafish Phenotypes
DiGeorge	*TBX1*	TOF, PA-VSD, truncus arteriosus, IAA, aortic arch anomalies, VSD	Impaired cardiac jogging and looping, aortic arch defects, reduced proliferation in FHF, reduced incorporation of SHF cells at arterial pole, impaired OFT development
Williams-Beuren	*ELN*	SVAS, pulmonary arterial stenosis, STA, PPS, OFT obstruction	Hypoplasia and reduced contraction of the BA, aberrant cardiac/smooth muscle differentiation
Holt–Oram	*TBX5*	ASD, VSD, TOF, arrhythmias, HLHS, PDA	Impaired cardiac looping, arrested differentiation, reduced contractility, stretching (and ripping) of atrium, smaller ventricle

ASD: atrial septal defect; *AVSD*: atrioventricular septal defect; *BA*: bulbus arteriosus; *CoA*: coarctation of the aorta; *DORV*: double outlet right ventricle; *HCM*: hypertrophic cardiomyopathy; *HLHS*: hypoplastic left heart syndrome; *IAA*: interrupted aortic arch; *LVOTO*: left ventricular outflow tract obstruction; *OFT*: outflow tract; *PA-VSD*: pulmonary atresia with VSD; *PDA*: persistent ductus arteriosus; *PPS*: peripheral pulmonary stenosis; *PS*: pulmonary stenosis; *PVS*: pulmonary valve stenosis; *RVOTO*: right ventricular outflow tract obstruction; *STA*: stenosis of the thoracic aorta; *SVAS*: supravalvular aortic stenosis; *TOF*: tetralogy of fallot; *VSD*: ventricular septal defect.

2. ZEBRAFISH HEART DEVELOPMENT

Although occurring on a much faster scale, the processes driving zebrafish heart formation are very similar to those described for other vertebrates. In brief, in vertebrates the heart is formed from mesodermal cells that are specified during gastrulation on both the left and right sides of the embryo. These cells undergo similar processes including differentiation, medial migration to the midline, and fusion of both left and right populations at the midline to form a contractile heart tube. Additional cells are subsequently recruited from a secondary heart field to the poles of the heart tube, where they contribute to structures including the myocardium

and the outflow tract (OFT). The heart tube bends rightward in a process known as cardiac looping, which, in humans, is necessary for alignment and septation of the cardiac chambers (Harvey & Rosenthal, 1999). The bending of the linear tube during cardiac looping in zebrafish is preceded by an asymmetric process termed "jogging," whereby the atrial cells are placed to the anterior and left of ventricular cells during generation of the linear tube. Despite differences, the genes and mechanisms involved in cardiac development are conserved between zebrafish and humans, and are presented in more detail below.

2.1 Specification and Differentiation of Cardiac Progenitor Cells

The first step in cardiac development is the specification of cells as CPCs. Labeling of individual blastomeres using laser-mediated activation of caged fluorescein revealed that by 5 h postfertilization (hpf), myocardial populations are specified as either ventricular or atrial precursors (Fig. 1A; Keegan, Meyer, & Yelon, 2004). Both populations reside in the lateral marginal zone (LMZ), an area of developing mesendodermal cells at the border between the cells and the yolk, with ventricular precursors located more dorsally and marginally. Endocardial precursors reside in the LMZ alongside myocardial cells (Fig. 2A), but are not spatially segregated into ventricular and atrial populations at this stage (Keegan et al., 2004). After their involution during gastrulation, precursor cells migrate to the anterior lateral plate mesoderm (ALPM), where they form distinct bilateral sheets on either side of the midline by 15 hpf, with ventricular precursors located more medially than atrial progenitors (Fig. 1B–D; Yelon, Horne, & Stainier, 1999).

Multiple signaling pathways converge to regulate CPC specification. Hedgehog (Hh) signaling acts cell autonomously to promote both ventricular and atrial CPC specification, while retinoic acid (RA) acts to restrict the number of cardiac progenitors. Wnt signaling acts biphasically, with induction or repression of specification dependent on whether signaling is active before, or during, gastrulation, respectively. Subpopulation-specific effects are also evident; ventricular CPCs are more sensitive to regulation by Nodal and fibroblast growth factor (FGF) signaling than atrial CPCs, while atrial precursors are more affected by changes in bone morphogenetic protein (BMP) signaling than ventricular precursors (for a more in depth review of signaling in CPC development, see Staudt & Stainier, 2012).

Cardiomyocyte differentiation is driven by a variety of transcription factors. Both pools of myocardial CPCs express *nkx2.5* (Yelon et al., 1999), and

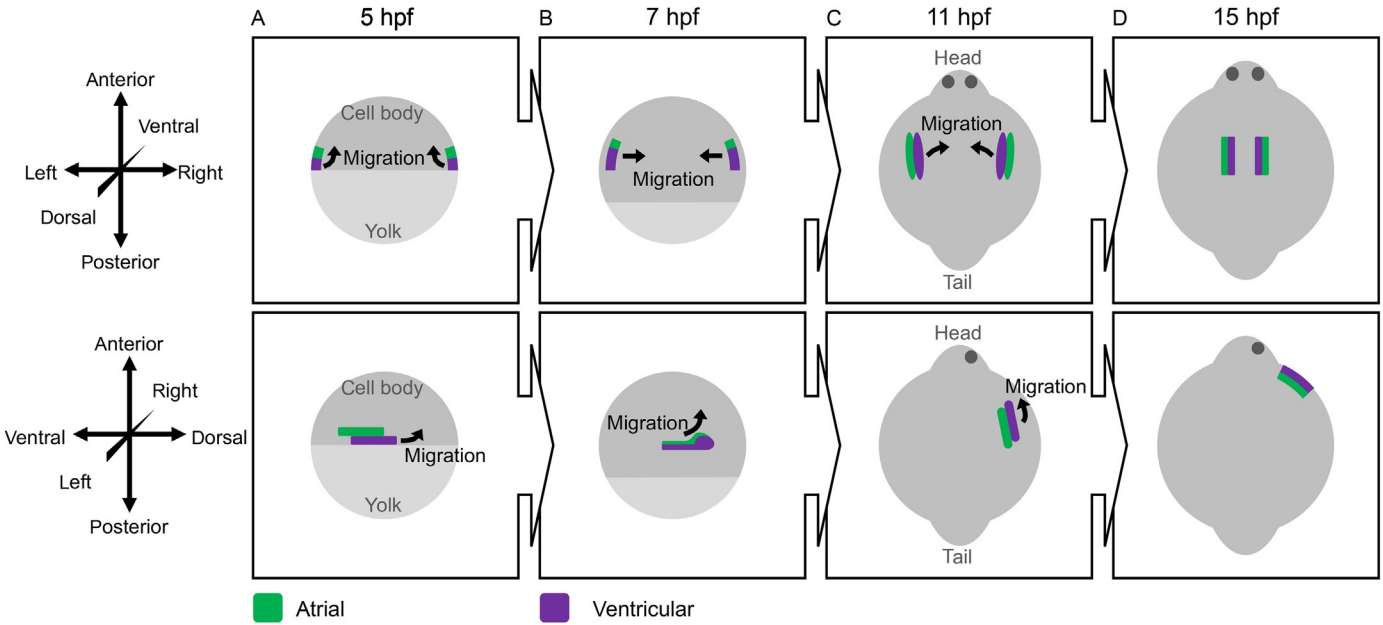

Fig. 1 Specification and migration of cardiac precursor cells. (A) Atrial and ventricular cardiac progenitor cells (CPCs) are specified on both the left and right side of the embryo. Ventricular precursors lie dorsal and marginal to atrial precursors. (B) CPCs maintain their relative spatial organization while migrating dorsally as cohesive sheets. (C) CPCs migrate toward the embryonic midline, such that atrial progenitors are lateral and ventral to ventricular precursors. (D) This organization is maintained during migration to the anterior lateral plate mesoderm.

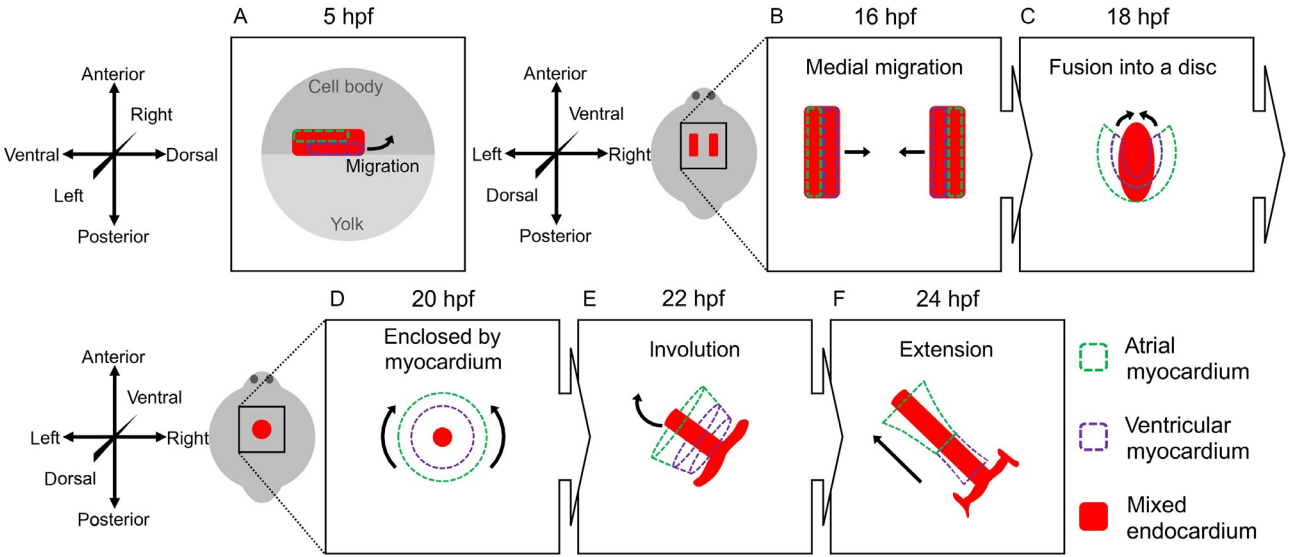

Fig. 2 Endocardial development and migration. (A) Endocardial precursors originate in the lateral marginal zone but show no separation into atrial and ventricular subpopulations. (B) Bilateral populations of endocardial cells initiate medial migration at 16 hpf. (C) Endocardium coalesces into a disk in the embryonic midline. (D) Myocardial fusion initiates at the posterior of the endocardial disk and proceeds to enclose the endocardium. (E) During jogging, the endocardium involutes with the myocardium. (F) The endocardium lines the lumen of the myocardial tube.

loss of *nkx2.5* and *nkx2.7* disrupts heart tube assembly, resulting in excess atrial cells at 26 hpf and reduced ventricular cardiomyocytes by 52 hpf (Targoff et al., 2008). Loss of both Gata5 and Gata6 results in reduced CPCs (Holtzinger & Evans, 2007) and minimal differentiated myocardial tissue develops in mutants for *hand2*, the basic helix-loop-helix transcription factor (Yelon et al., 2000). All CPCs express *myosin light chain* 7 (*myl7*), but subpopulations can be distinguished since ventricular cardiomyocytes express *ventricular myosin heavy chain* (*vmhc*) while atrial cardiomyoctyes express *atrial myosin heavy chain* (*amhc*) (Yelon et al., 1999).

2.2 Heart Tube Formation and Extension

Heart tube development requires the medial migration of bilateral populations of endocardial and myocardial CPCs. The endocardial cells initiate migration at 16 hpf (14 somites, Fig. 2B) and move posteriorly (Bussmann, Bakkers, & Schulte-Merker, 2007). Fusion of the populations is initiated at 16.5 hpf (15 somites) and completed by 18 hpf (18 somites), when the endocardium forms a disk at the embryonic midline (Fig. 2C). Endocardium development is incompletely understood, but the transcription factor Tal1 is involved. Tal1 gain-of-function leads to expansion of the endothelial population, while loss-of-function causes aggregation of endocardial cells at the arterial pole of the heart, inducing ventricular stenosis (Bussmann et al., 2007; Gering, Yamada, Rabbitts, & Patient, 2003). *cloche*, a bHLH-PAS transcription factor, acts upstream of Tal1 as a master regulator of endothelial specification and its mutation leads to loss of endocardium (Reischauer et al., 2016). Medial migration is also influenced by vascular endothelial growth factor. Increasing the response to this important factor by modulating Slit/Robo signaling leads to multiple heart lumens as a result of faster movement of individual cells at the expense of collective migration. Decreasing the response to this factor causes unfused heart fields as a consequence of inhibited migration (Fish et al., 2011).

Endocardial CPC migration is essential in forming the endocardium, but also facilitates morphogenesis of the myocardium. Endocardial loss causes myocardial dysmorphia, as in the *cloche* mutant where angular cardiomyocyte migration is incorrectly executed (Holtzman et al., 2007; Stainier et al., 1995). This crosstalk is reciprocal, as when myocardial cells are reduced in number by deletion of *hand2*, endocardial cells migrate properly but fail to form the cardiac cone, seemingly as a consequence of disrupting BMP signaling (Garavito-Aguilar, Riley, & Yelon, 2010;

Palencia-Desai et al., 2015). Similarly, myocardial Tmem2 promotes migration of both myocardial and endocardial CPCs, with loss delaying medial migration of both populations and endocardial populations ultimately failing to fuse (Totong et al., 2011).

Myocardial CPCs begin medial migration to the midline later than endocardial cells, at 17.5 hpf (17 somites), as revealed through a combination of in situ hybridization, fate mapping, and live cell imaging experiments using fluorescently tagged cell type markers (Holtzman et al., 2007; Stainier et al., 1996; Yelon et al., 1999). Fusion initiates at the posterior end of the myocardium at 18 hpf (18 somites), with ventricular CPCs making contact prior to atrial CPCs (Fig. 3B). Myocardial fusion occurs immediately anterior to the most posterior endocardial cells (Fig. 2C). A second phase of angular migration allows the cardiomyocytes to surround the central endocardial cells (Fig. 2D) (Holtzman et al., 2007). Anterior myocardial CPCs then fuse to form a shallow cone (Fig. 3C) where ventricular precursors form the apex and atrial precursors localize beneath them at the wider base by 20 hpf (22 somites). The central lumen is lined with those endocardial cells that will connect to the aortic arches, although most of the endocardium remains ventral to the myocardial cardiac cone (Holtzman et al., 2007; Stainier, Lee, & Fishman, 1993).

The myocardial cells are organized into a single-layered epithelium, where ventricular CPCs adopt a cuboidal morphology and atrial CPCs are more squamous (Rohr, Bit-Avragim, & Abdelilah-Seyfried, 2006; Rohr, Otten, & Abdelilah-Seyfried, 2008). Proper cone formation requires cells to maintain their epithelial integrity. Mutations disrupting the adherens or tight junctions, such as *prkci* in *heart-and-soul* (*has*) or *mpp5a* in *nagie oko* (*nok*), impact cone formation (Horne-Badovinac et al., 2001; Peterson, Mably, Chen, & Fishman, 2001; Rohr et al., 2006, 2008). In *has* mutants, myocardial CPCs exhibit delayed posterior fusion until after the anterior regions have coalesced, and this delay causes a failure of tube morphogenesis with ventricular tissue developing within the atrium. CPCs do fuse at the midline in *nok* mutants, but the myocardial layer loses epithelial coherence, forming partial multilayers, and failing to undergo cone rotation. Epithelial integrity is also important during subsequent stages of cardiac morphogenesis. Disruption of cell junctions results in nondirectional migration of single cells that have lost contact with the surrounding cells (Rohr et al., 2008). Thus, epithelial coherence ensures cells migrate collectively, move uniformly in the correct direction, and maintain contact with neighboring cells to prevent population mixing.

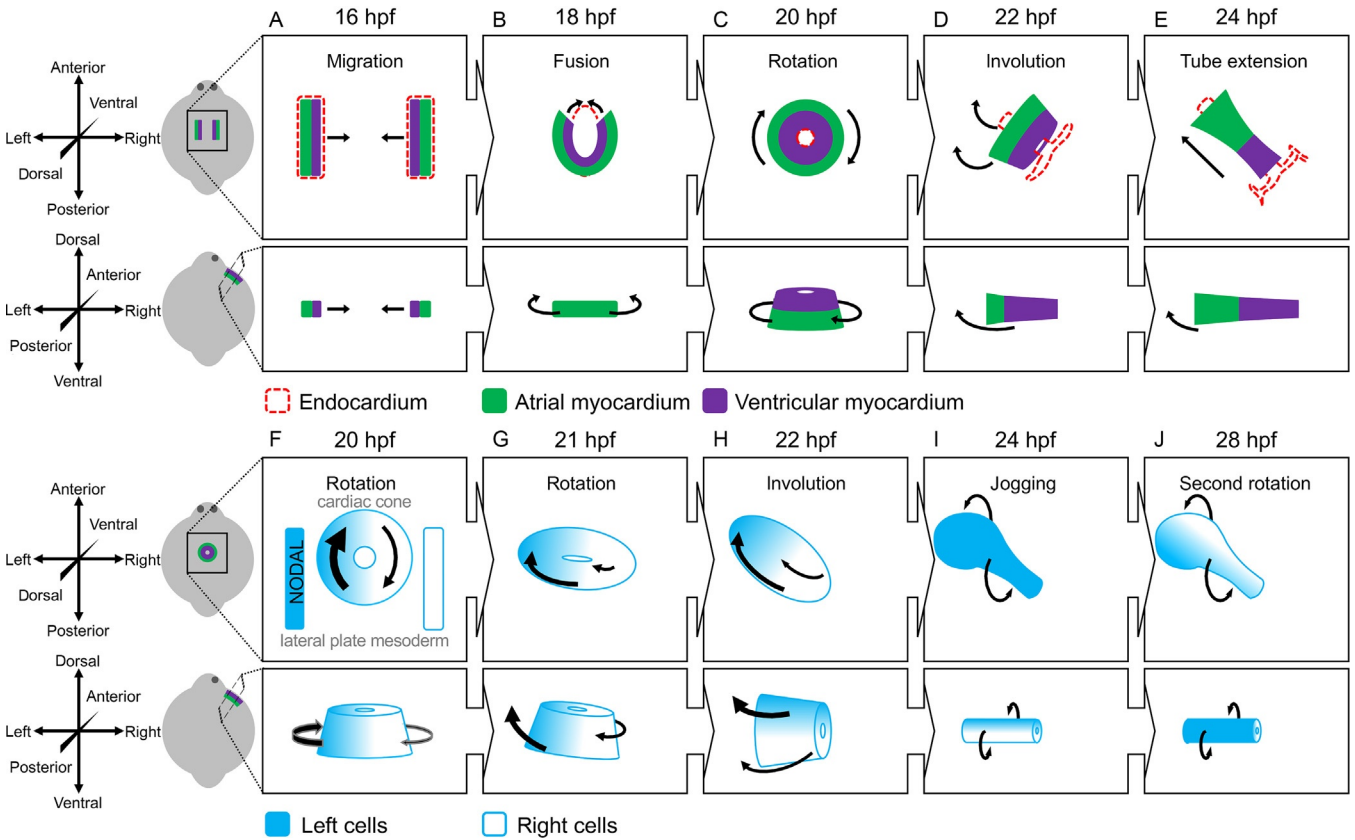

Fig. 3 See legend on next page.

Successful migration of CPCs additionally depends on input from the endoderm and extracellular matrix (ECM). The endoderm contributes a surface along which CPCs can migrate and actively signals to the myocardium, for example through sphingolipids (Fukushima, Ishii, Contos, Weiner, & Chun, 2001; Maceyka, Payne, Milstien, & Spiegel, 2002). Mutations in the transcription factors *gata5* and *sox32*, or the Nodal cofactor *oep*, result in loss of endoderm tissue and a failure of CPCs to migrate to the midline. Mutation of the *sphingosine-1 phosphate receptor* (*s1pr2*) or the sphingosine-1 phosphate transporter *spinster 2* (*spns2*) disrupts sphingolipid signaling and causes similar CPC migration phenotypes. The result is cardia bifida, in which two separate hearts develop on either side of the midline (Hisano, Ota, Takada, & Kawahara, 2013; Kawahara et al., 2009; Kupperman, An, Osborne, Waldron, & Stainier, 2000; Osborne et al., 2008; Stainier et al., 1996). The finding that cardia bifida also occurs in mutants where fibronectin deposition is altered, blocking migration of the CPCs toward the midline, demonstrates the importance of the ECM in directing the location and formation of the heart (Arrington & Yost, 2009; Sakaguchi, Kikuchi, Kuroiwa, Takeda, & Stainier, 2006; Trinh & Stainier, 2004; Yelon et al., 2000).

Once the cardiac cone forms it continues to migrate as a collective population culminating in the conversion of the cone into a linear heart tube. This process, called "jogging" in zebrafish, is influenced by left–right patterning cues generating the first morphological visceral asymmetry in the embryo. Jogging occurs over the span of 4 h and culminates in asymmetric positioning of the atrium to the left and anterior of the ventricle (Figs. 2E and F and 3D and E). The entire process can be visualized by live imaging of

Fig. 3 Formation and positioning of the linear heart tube. (A) Cardiac precursors are localized to the anterior lateral plate mesoderm (ALPM), with ventricular precursors situated more medially than atrial precursors. (B) Populations migrate toward the midline, initiating contact at the posterior. (C) Anterior fusion forms a shallow cone, with ventricular precursors forming the tip and atrial precursors forming the base. (D) The cone rotates, tilting such that atrial cells are to the left of ventricular cells. (E) Cone extension positions atrial cells to the left and anterior of ventricular populations. (F) Nodal signaling from the left LPM increases the migratory velocity of cells on the left of the cardiac cone, resulting in clockwise rotation. (G) Left cells migrate left anteriorly along the lateral edges of the cone while slower cells on the right migrate anteriorly around the lumen of the cone. (H) During later stages of rotation the cone tilts in addition to rotating. (I) Cells originating on the left are displaced to form the dorsal region of the extending heart tube. (J) An additional leftward rotation occurs to reposition cells originating from the left and right cells back to their respective sides of the extending tube.

fluorescently tagged cardiomyocytes and in situ hybridization (for example, see Baker, Holtzman, & Burdine, 2008; de Campos-Baptista, Holtzman, Yelon, & Schier, 2008; Rohr et al., 2008; Smith et al., 2008) providing detailed characterization of cell behavior. The jogging direction of the heart is regulated by asymmetric Nodal signaling (Fig. 3F). The zebrafish Nodal gene *southpaw* (*spaw*) is expressed in the left lateral plate mesoderm (LPM) but is absent from the right LPM (Baker et al., 2008; Long, Ahmad, & Rebagliati, 2003; Schier & Shen, 2000). Live imaging revealed that exposure to Nodal signaling increases the velocity of CPC migration in the left side of the cardiac cone, compared to the right (Baker et al., 2008; de Campos-Baptista et al., 2008; Lenhart, Holtzman, Williams, & Burdine, 2013; Smith et al., 2008). This left–right (L–R) asymmetry in CPC migration velocity causes the cardiac cone to rotate clockwise as the entire cone migrates anteriorly (Fig. 3G). This rotation is accompanied by involution of cells on the posterior right of the midline (Fig. 3H), leading to tilting of the cone along the anterior posterior axis (Rohr et al., 2008). Together, asymmetric cell migrations and involution cause the tube to extend toward the left into the typical leftward jog (Fig. 3I). In the absence of *spaw*, CPC migration velocities are significantly slowed and become more L–R symmetrical. In addition, the point of involution within the cone becomes randomized. Together this leads to loss of left jogging, and heart tube positioning along the L–R axis becomes random in direction (Lenhart et al., 2013; Rohr et al., 2008; Smith et al., 2008).

While it is clear Nodal signaling is the dominant laterality cue in the heart, BMP signaling also plays a role in jogging laterality though the exact role remains to be determined (Lenhart et al., 2013; Smith et al., 2008; Veerkamp et al., 2013). Migration of CPCs toward exogenous BMP protein suggests this molecule can function as a promigratory cue (Smith et al., 2008). However, Bmp activity is reported to be higher on the right in slower migrating cells (Veerkamp et al., 2013). Additionally, mutations in *bmp4* suggest a role for limiting cell velocity of CPCs (Lenhart et al., 2013). Given that heterozygous mutants for *bmp4* could modify the phenotypes observed in *spaw* morphants, the levels of BMP signaling may be critical for proper CPC migration (Lenhart et al., 2013). Interestingly, the response to BMP signaling, as visualized by phospho-SMAD 1/5/8 immunoreactivity, appears to be within the endocardium. The BMP response in this tissue is abolished with the Nodal transcription factor FoxH1 is mutated, further suggesting Nodal signaling lies upstream of the BMP response (Lenhart et al., 2013).

As a result of rotation and involution, cells from the left half of the cone that received Nodal signals from the LPM localize to the dorsal side of the heart tube (Baker et al., 2008; Rohr et al., 2008). A second, leftward rotation occurs to reposition the dorsally displaced cells back to the left of the heart tube by 48 hpf, prior to cardiac looping (Fig. 3J; Baker et al., 2008), but the mechanisms involved remain to be clarified.

Overall, the role of Nodal in directing asymmetric cardiac morphogenesis is conserved among vertebrates, although the exact event influenced by this pathway is organism specific. In mouse for example, *Nodal* is asymmetrically expressed just prior to cardiac looping and influences the directionality of this process. In zebrafish, Nodal is expressed lateral to the cardiac cone and influences cone rotation and jogging as described earlier. Additionally, cardiac cone rotation in zebrafish seems analogous to the slight rotation observed in the linear heart tube during looping in mouse and chick (Baker et al., 2008; Rohr et al., 2008; Smith et al., 2008).

Following its formation, the heart tube undergoes extension. Elongation is not a result of increased proliferation, as the cardiomyocyte proliferation rate is very low (de Pater et al., 2009; Rohr et al., 2006). At 20 hpf (22 somites) the cardiac cone comprises approximately 85 cells (R. Burdine, unpublished). By 24 hpf, the heart tube is approximately 150 cells, growing to 270 cells by 36 hpf and 310 cells by 48 hpf (de Pater et al., 2009; Rohr et al., 2006). Such low proliferation rates are insufficient to account for the increases in tube length. Instead, the cone is lengthened by remodeling myocardial cell morphology, such that cells—especially atrial precursors—adopt an extended squamous morphology, and by addition of cells from secondary sources (de Pater et al., 2009; Hami, Grimes, Tsai, & Kirby, 2011; Rohr et al., 2006).

2.3 The Second Heart Field

Two fields of CPCs form the vertebrate heart. The first heart field (FHF) gives rise to the linear heart tube (Fig. 3). The evolutionarily conserved second heart field (SHF) contributes CPCs that are progressively added to the poles of the heart tube. SHF progenitors remain undifferentiated in pharyngeal mesoderm until incorporated into heart tube myocardium between 24 and 48 hpf, where they are added to either the arterial (outflow) pole at the ventricular end of the heart tube (Fig. 4A and B) or to the venous pole (inflow tract) at the atrial end (de Pater et al., 2009; Hami et al., 2011). SHF cells contribute to smooth muscle in the OFT, also referred to as the bulbus

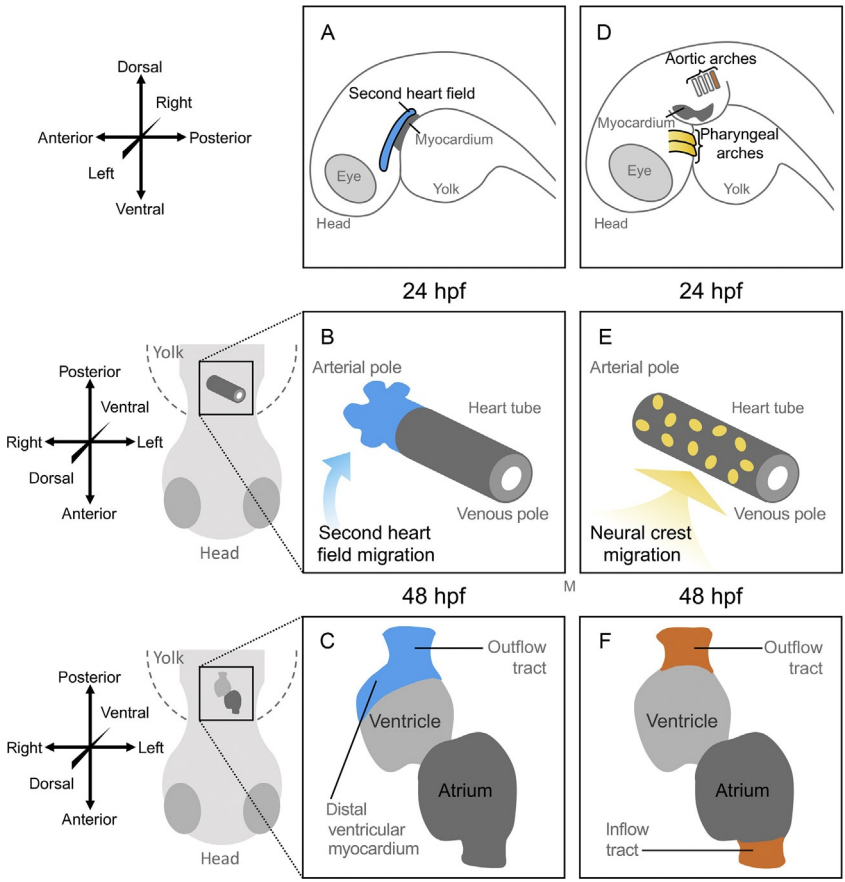

Fig. 4 Secondary cardiac precursor populations contribute cells to different regions of the developing heart. (A) The second heart field (SHF) overlies the proliferating myocardium, localizing to the pharyngeal arches. (B) SHF cells contribute to the arterial pole. (C) Later in development, SHF cells localize to distal ventricular myocardium and the outflow tract. (D) Cardiac neural crest cell (CNC) arise from between rhombomeres 1 and 6 (not shown). Early streaming CNC migrate through pharyngeal arches 1 and 2. Later streaming CNC migrates through aortic arch 6. (E) Early migrating CNC contribute cardiomyocytes throughout the linear heart tube. (F) Later migrating CNC populate the inflow and outflow tracts.

arteriosus (BA) in zebrafish, as well as the distal ventricular myocardium (Fig. 4C) (Grimes et al., 2006; Hami et al., 2011; Zhou et al., 2011).

Multiple transcription factors have been identified as SHF regulators in zebrafish. For example, knockdown of *tbx1*, *mef2c*, or *nkx2.5* impairs SHF cell proliferation and differentiation, and underdevelopment of

SHF-derived structures, including the OFT and distal ventricular myocardium (Guner-Ataman et al., 2013; Hinits et al., 2012; Lazic & Scott, 2011). SHF accretion to the arterial pole requires FGF and TGFβ signaling; pharmacological inhibition of FGF signaling or knockdown of latent TGFβ-binding protein 3 (Ltbp3) results in decreased accretion at the arterial pole and truncation of the OFT (Marques, Lee, Poss, & Yelon, 2008; Zhou et al., 2011). These defects are consistent with human conotruncal heart defects, which can arise from defective SHF development and comprise nearly 30% of all CHDs (Rochais, Mesbah, & Kelly, 2009). There are some interesting differences, however. For example, in mouse, the transcription factor Isl1 is required for the recruitment of cells to both the venous and arterial pole of the heart tube (Cai et al., 2003). In zebrafish, it is required for cardiomyocyte differentiation at the venous pole but not at the arterial pole (de Pater et al., 2009). Thus, since the SHF in zebrafish is akin in origin and function to that of mammals, studying SHF formation in zebrafish embryos can inform how SHF-related CHDs arise in humans.

2.4 Cardiac Neural Crest

Neural crest cells (NCCs) give rise to a large number of differentiated cell types and can be divided into five subtypes—cranial, vagal, sacral, trunk, and cardiac. In zebrafish, cardiac neural crest cells (CNCCs) invade the myocardium of many cardiac structures, including the OFT, atrium, ventricle, and atrioventricular canal (AVC) (Li et al., 2003; Sato & Yost, 2003). CNCCs originate in a broad region between rhombomeres 1 and 6, but their addition to the developing heart occurs in two waves as visualized by lineage tracing and fate mapping (Cavanaugh, Huang, & Chen, 2015; Sato & Yost, 2003). In the first stream, CNCCs migrate via pharyngeal arches 1 and 2 and are added throughout the heart tube between 24 and 30 hpf (Fig. 4D and E), where they differentiate into cardiomyocytes. In the second stream, CNCCs migrate via aortic arch 6 and are added to the ventral aorta and OFT around 80 hpf (Fig. 4D and F) (Cavanaugh et al., 2015). A variety of factors are involved in regulating CNCC contributions to the heart, including Wnt, FGF, and Semaphorin pathways (Cavanaugh et al., 2015; Sato, Tsai, & Yost, 2006; Sun, Zhang, Lin, & Xu, 2008).

Given the cellular contributions of CNCCs to different cardiac structures, it is unsurprising that defective CNCC development has been implicated in CHDs, including OFT malformations, ventricular septal defects

(VSDs), aortic arch anomalies, pulmonary stenosis (PS), and coarctation of the aorta (CoA) (Keyte & Hutson, 2012). Disrupting CNCCs in zebrafish also causes cardiac defects including compromised cardiac looping, depressed heart rate, smaller ventricles, and loss of SHF cell recruitment (Cavanaugh et al., 2015; Li et al., 2003), making fish a useful model for pursuing the role of CNCCs in cardiac disease.

2.5 Cardiac Looping, Ballooning, and Chamber Formation

The heart tube bends rightward in a process known as cardiac looping, which, in humans, is necessary for alignment and septation of the cardiac chambers (Harvey & Rosenthal, 1999). Though the zebrafish heart chambers are not septated, cardiac looping is still occurs. Looping begins at 30 hpf, forming a slight kink in the middle of the linear tube (Fig. 5A). Bending becomes more pronounced, with the tube becoming increasingly "S" shaped as development proceeds (Fig. 5B). Looping occurs in a defined L–R asymmetric fashion, resulting in a dextral loop that positions the ventricle to the right and anterior of the atrium. The events underlying looping morphogenesis remain poorly understood, although cellular migration and tissue-level forces exerted through the cytoskeleton are likely to be involved. Treatment of explanted linear heart tubes with cytochalasin B or blebbistatin, inhibitors of actin polymerization and myosin II, respectively, impairs cardiac looping and constriction at the AVC (Noel et al., 2013).

Following looping, heart chambers expand via cardiac ballooning (Fig. 5C). During this process, the chamber curvatures can be distinguished by the expression of *naturietic peptide precursor a* (*nppa*), which is regionally restricted to the myocardium of the convex outer curvature (OC) of both chambers, but absent from the concave inner curvature (IC) and AVC (Auman et al., 2007). OC cells appear elongated and flattened, while cells of the IC remain cuboidal, suggesting that regionalized differences in cell morphology bring about curvature formation and chamber expansion (Fig. 5C and D). The enlargement and elongation of OC cells are stimulated by blood flow but restricted by contractility (Auman et al., 2007). For example, *weak atrium* (*wea*) mutants exhibit decreased blood flow through the ventricle, resulting in OC cells that are smaller and less elongated than normal (Auman et al., 2007). Pharmacological reduction of blood flow has a similar effect on cardiomyocyte morphology. Conversely, ventricular cardiomyocytes in *half-hearted* (*haf*) mutants, in which ventricular contractility is defective, are overly enlarged and elongated.

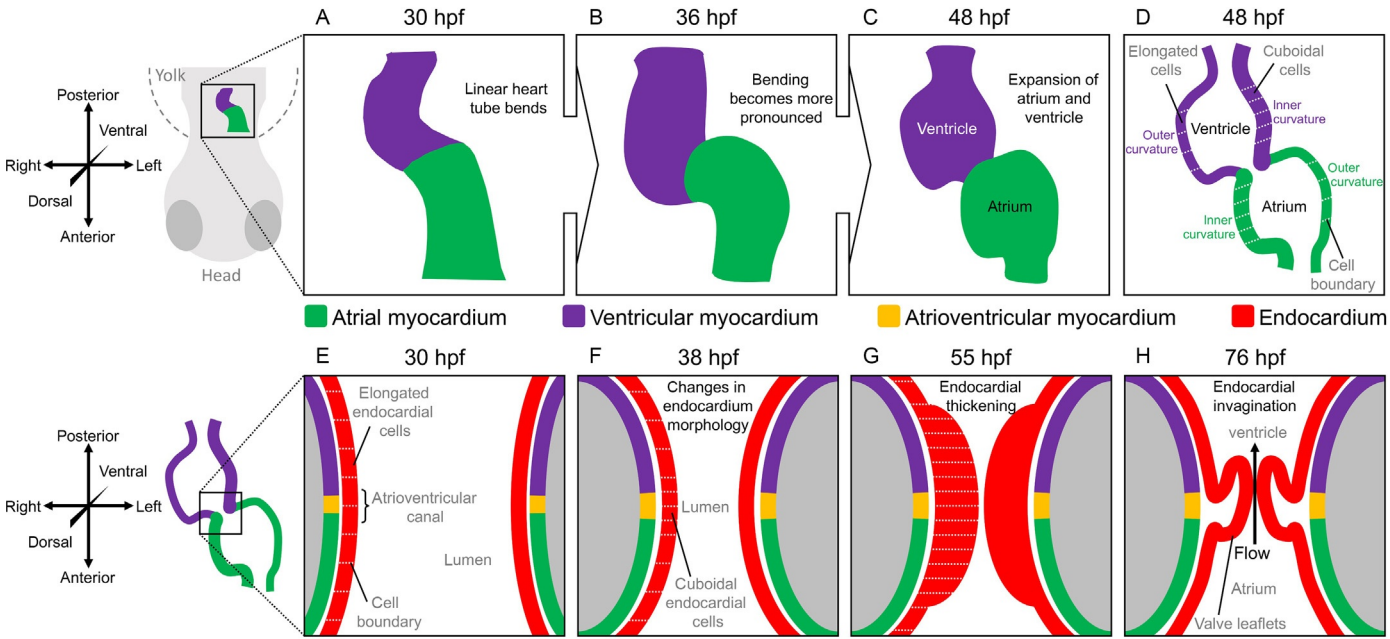

Fig. 5 Transforming the linear tube into a functional heart. (A) Looping begins with bending of the linear tube to form a slight "S" shaped tube. (B) Looping becomes more pronounced and the "S" shape more prominent. (C) The atrium and ventricle expand to become discernible chambers during ballooning. (D) Expansion requires changes in cell morphology, where cells in the inner curvature remain cuboidal while cells in the outer curvature are elongated and flattened. (E) During valve formation, the atrioventricular myocardium (AVC) forms the boundary between the ventricular and atrial regions. (F) Endocardial cells adjacent to the AVC change morphology from elongated to cuboidal. (G) The increasing cell morphology changes result in thickening of the endocardium in the AVC region. (H) Invagination of the endocardium forms unidirectional valves.

2.6 Valvulogenesis

The linear heart tube drives circulation by acting as a suction pump. Contractions of the linear heart tube result in systemic distribution of blood with little regurgitation, even though there are no valves. However, the looped heart is an ineffective suction pump with substantial backflow (Forouhar et al., 2006; Liebling et al., 2006). Thus, dextral looping and growth of the heart necessitate the development of valves in the AVC that reestablish unidirectional flow (Liebling et al., 2006; Scherz, Huisken, Sahai-Hernandez, & Stainier, 2008). The AVC arises as a constriction at the boundary between the chambers during cardiac looping (Fig. 5E). Cells within the AVC begin differentiating at 36 hpf, a time when most endocardial cells are squamous in shape, but a few at the boundary between the chambers appear cuboidal (Fig. 5F) and express different markers, such as DM-GRASP (Beis et al., 2005). By 55 hpf, endocardial cells lining the AVC form a pronounced layer of cuboidal cells (Fig. 5G) and then leaflets form through invagination of AVC endocardium (Fig. 5H). These leaflets ultimately function to prevent backflow (Scherz et al., 2008). At the same time, because of apical membrane constriction, AVC myocardial cells become trapezoidal in morphology (Chi et al., 2008).

Cardiac function is critical for proper valvulogenesis. In the *silent heart* (*sih*) mutant, where mutation of *cardiac troponin T* (*tnnt2*) causes lack of heartbeat and circulation, endocardial cells lack expression of DM-GRASP, remain squamous in morphology, and do not constrict at the AVC (Bartman et al., 2004; Beis et al., 2005). Analysis of *sih* and pharmacological reduction of myocardial force suggests that AVC development is more sensitive to defects in contraction and blood flow directionality, than to shear stress (Bartman et al., 2004; Vermot et al., 2009).

In humans, defective valve formation manifests as aortic valve stenosis, mitral valve prolapse (MVP), calcific aortic valve disease, pulmonary valve stenosis (PVS), Ebstein's anomaly, or bicuspid aortic valve (BAV). Studies in zebrafish have already proven useful in dissecting the genetics underlying these defects. Deregulated Notch or BMP signaling, or activation of RAS/mitogen-activated protein kinase (MAPK) signaling, contribute to valve defects in both human patients and zebrafish, demonstrating the promise of zebrafish models in understanding human valve disease (LaHaye, Lincoln, & Garg, 2014; Padmanabhan et al., 2009; Peal, Lynch, & Milan, 2011; Rose, Force, & Wang, 2010).

3. ZEBRAFISH MODELS OF SYNDROMIC CHD

Considering the complexity of heart development, it is unsurprising that CHDs are so common in humans; failure in any of the precise progressive steps can derail development, resulting in malformation and/or dysfunction. Mutations can impinge on heart development alone or generate a spectrum of defects that comprise developmental syndromes, arising from a monogenic change (Table 1 and discussed throughout the text) or a multigenic mechanism. We discuss a subset of developmental syndromes that include CHDs as a major or defining feature, and arise from a range of primary causes. Modeling these syndromes often recapitulates the pleiotropic symptoms observed in patients, but here we focus on the cardiac aspects of these syndromes.

3.1 Left–Right Asymmetry and CHDs

The vertebrate heart exhibits L–R asymmetry in both the placement of the heart and the pattern of chambers and vessels. L–R asymmetry originates at midline structures called L–R coordinators (LRCs); Kupffer's vesicle (KV) in zebrafish (Amack, 2014; Blum, Weber, Beyer, & Vick, 2009). Cells within LRCs bear motile cilia, small microtubule-based organelles protruding from the apical surface, which beat or rotate to drive asymmetric fluid flow and elicit asymmetries in gene expression (Yoshiba & Hamada, 2014).

In mouse, flow is detected by sensory cilia around the LRC in a mechanism that involves Polycystin proteins (Norris & Grimes, 2012). The polycystins Pkd1l1 and Pkd2 also play a role in L–R patterning in fish, although it is yet unknown whether cilia are required for flow sensation in KV (Bisgrove, Snarr, Emrazian, & Yost, 2005; Kamura et al., 2011; Schottenfeld, Sullivan-Brown, & Burdine, 2007). Flow sensation culminates in *nodal* (*spaw*) expression in the left LPM only, and Nodal signaling activates the homeodomain transcription factor Pitx2 in the left LPM (Hamada & Tam, 2014). While Pitx2 is a primary target of Nodal signaling on the left, the role of Pitx2 in early asymmetric cardiac morphogenesis appears minimal, although it may play later roles in asymmetries in the OFT in mice (Ai et al., 2006; Yashiro, Shiratori, & Hamada, 2007). Although in *Xenopus* and chick misexpression of *pitx2* in the right LPM reverses heart looping, in zebrafish *pitx2* mutants heart jogging and looping occurs normally (Ji, Buel, & Amack, 2016; Levin et al., 1997; Ryan et al., 1998; Sampath, Cheng, Frisch, & Wright, 1997). Looping also occurs

normally in mouse mutants, suggesting *Pitx2* is dispensable for this event (Gage, Suh, & Camper, 1999; Lin et al., 1999; Lu, Pressman, Dyer, Johnson, & Martin, 1999).

Disruption of L–R asymmetry causes CHDs, including transposition of the great arteries (TGA), double outlet right ventricle (DORV) and persistent truncus arteriosus (Ramsdell, 2005). Given their importance in generating heart asymmetry, it is unsurprising that mutations disrupting ciliary structure or function, resulting in ciliopathies, commonly involve CHDs (Ramsdell, 2005). CHDs are particularly prevalent in primary ciliary dyskinesia (PCD), a subset of ciliopathies caused by cilia motility defects (Li et al., 2015; Zariwala, Omran, & Ferkol, 2011), and in heterotaxy, a rare condition characterized by discordant placement of organs resulting from L–R defects (Icardo & Sanchez de Vega, 1991; Nakhleh et al., 2012; Sutherland & Ware, 2009). Many potentially causative heterotaxy genes have been identified by sequencing patient cohorts and model organism genetic screens (Fakhro et al., 2011; Guimier et al., 2015; Li et al., 2015). Investigation of the specific role played by these genes in model organisms like zebrafish, where the stages of L–R patterning are particularly well understood, will be critical for understanding how human sequence variants cause disease (Fakhro et al., 2011). Interestingly, mutations in *PKD1L1* and *PKD2*, required for L–R patterning in zebrafish, cause heterotaxy with CHD in humans (Bataille et al., 2011; Bisgrove et al., 2005; Schottenfeld et al., 2007; Vetrini et al., 2016). Conversely, it is important to assess whether L–R patterning genes identified in zebrafish contribute to heterotaxy and/or CHD in humans.

3.2 CHARGE Syndrome

CHARGE syndrome (*C*oloboma, *H*eart defects, *A*tresia choanae, *R*etarded growth/development, *G*enital abnormalities, and *E*ar anomalies/deafness) affects 1 in 10,000 individuals (Blake & Prasad, 2006). CHDs are found in 75–85% of CHARGE patients and are a major cause of mortality (Zentner, Layman, Martin, & Scacheri, 2010).

Several genes associated with CHARGE syndrome have been discovered to be important for zebrafish heart development. For instance, *Chromodomain helicase DNA-binding protein-7* (*CHD7*) haploinsufficiency causes CHARGE syndrome (Vissers et al., 2004; Zentner et al., 2010), and knockdown of *chd7* in zebrafish results in defects reminiscent of those of CHARGE patients. *chd7* morphants display heart defects including

dysmorphic cardiac chambers and pericardial edema (Balow et al., 2013; Patten et al., 2012). Blood flow and heartbeat are also reduced, resembling the cardiac rhythm abnormalities of CHARGE patients (Blake & Prasad, 2006; Roger et al., 1999). CHD7 localizes and remodels chromatin in human cell lines, associating with activating methylation marks, implicating epigenetic misregulation in the development of CHDs (Schnetz et al., 2009).

Roughly two-thirds of CHARGE syndrome patients have a mutation in CHD7. Although the genetic cause remains to be discovered for some patients, others have mutations in genes known to be important for heart development. For example, mutations in *SEMA3E* and *SEMA3A* were found in a subset of CHARGE patients, but the role of these Semaphorins in disease development is unclear (Lalani et al., 2004; Schulz et al., 2014). However, zebrafish studies suggest that Semaphorins govern vascular angioblast migration and dorsal aorta formation (Shoji, Isogai, Sato-Maeda, Obinata, & Kuwada, 2003). Overexpression or knockdown of *sema3a* causes heart swelling, loss of circulation, and narrowing of the dorsal aorta in zebrafish, reminiscent of CoA in CHARGE patients (Shoji et al., 2003; Wyse, al-Mahdawi, Burn, & Blake, 1993). Thus, studies in zebrafish substantiate the argument that mutations in Semaphorins may cause CHARGE syndrome. Studies such as these demonstrate how zebrafish can be useful for assessing variants of unknown function associated with CHD.

3.3 Holt–Oram Syndrome

Patients with Holt–Oram syndrome (HOS) exhibit a combination of CHDs and upper limb defects (Holt & Oram, 1960). Affecting 1 in 100,000 individuals, 85% of HOS patients present with CHDs, most commonly atrial septal defects (ASDs), VSD, and conduction defects, and prognosis depends on the severity of the associated CHDs (Basson et al., 1994; Chryssostomidis et al., 2014).

HOS is caused by haploinsufficiency of *TBX5*, a T-box family transcription factor expressed throughout cardiac development (Hatcher, Goldstein, Mah, Delia, & Basson, 2000; McDermott et al., 2005). In the zebrafish *tbx5* mutant *heartstrings* (*hst*), differentiation arrests after 33 hpf and cardiac looping is impaired (Garrity, Childs, & Fishman, 2002). Contractility progressively decreases with a smaller ventricle and the atrium stretching and tearing (Garrity et al., 2002). *hst* mutants also exhibit decreased *camk2b2* expression in the heart and lower activity of CaMK-II (a target of calcium signaling), phenocopying patients with dilated cardiomyopathy and

conduction defects (Rothschild et al., 2009; Swaminathan, Purohit, Hund, & Anderson, 2012).

Although *TBX5* is the most frequently mutated gene in HOS, 25% of patients lack mutations in this gene. Mutations in genes regulated by TBX5 may cause HOS symptoms. For example, in some HOS patients, TBX5 mutations reduce expression of *MYH6*, a transcriptional target of TBX5 (Ching et al., 2005; Granados-Riveron et al., 2010). Moreover, mutations in *MYH6* itself cause several human heart defects, including ASD, although a direct link to HOS has not been established. Furthermore, zebrafish studies have demonstrated that Tbx5 synergizes with Mef2C, another transcription factor, to activate *myh6* transcription (Ghosh et al., 2009). Together with the fact that *mef2c* is essential for zebrafish heart development, these data suggest MEF2C function may also be critical in HOS pathology. In this way, probing molecular mechanisms in zebrafish may help inform the etiology of HOS by identifying new candidate genes for variant analyses in patient cohorts.

3.4 Cohesinopathies

Cohesin is a large multicomponent ring-shaped complex required for sister chromatid cohesion, whose function is governed by its ability to generate topological links between distant chromatin segments (Losada, 2014; Michaelis, Ciosk, & Nasmyth, 1997). Mutations in either core cohesin subunits or its regulators cause "cohesinopathies" (Watrin, Kaiser, & Wendt, 2016). Cohesinopathies encompass a broad spectrum of developmental abnormalities including CHDs such as VSD, ASD, PS, and tetralogy of fallot (TOF). Cornelia de Lange syndrome (CdLS), the best studied cohesinopathy, is frequently caused by heterozygous mutations in NIPBL, a protein critical for the loading of cohesin onto DNA, which cause misregulation of gene expression (Horsfield, Print, & Monnich, 2012; Krantz et al., 2004; Tonkin et al., 2004). *nipbl* depletion in zebrafish induces heart and gut defects, reminiscent of those observed in patients (Muto, Calof, Lander, & Schilling, 2011). The expression of genes controlling endodermal differentiation and L–R patterning is altered upon *nipbl* knockdown, and embryonic defects are caused by additive, synergistic interactions between misregulated genes (Muto et al., 2011).

The neural crest has also been implicated in heart defects in cohesinopathies. Depletion of the disease-associated cohesin subunit Rad21 led to smaller hearts, impaired looping, and valve defects in zebrafish (Deardorff et al., 2012; Schuster et al., 2015). Rather than contributing to

the heart, NCCs exhibited a "wandering" behavior linked to dysregulation of Wnt, chemokine, and cadherin genes (Schuster et al., 2015). These studies in zebrafish support the hypothesis that cohesinopathies result from the collective effect of multiple quantitative changes in the expression of developmental genes, rather than defects in chromosome segregation, and further suggest that mild mutations in cohesin subunits or regulators might underlie a higher-than-previously appreciated fraction of human CHDs.

3.5 RASopathies

Components of the RAS signaling pathway, a kinase cascade that activates MAPK, are mutated in the developmental syndromes termed RASopathies (Jindal, Goyal, Burdine, Rauen, & Shvartsman, 2015; Tidyman & Rauen, 2009). Mutations are generally thought to activate the pathway, and indeed, some mutations found in RASopathy patients can also be found in cancer lesions. Collectively occurring in 1 in 1000 births, individual RASopathy incidences range from 1 in 1500 for Noonan syndrome (NS), to 1 in 810,000 and 1 in 1,290,000 for the rare cardio-facio-cutaneous (CFC) syndrome and Costello syndrome (CS), respectively (Abe et al., 2012; Rauen, 2013).

CHDs are prevalent among RASopathies, with NS-associated mutations considered the most frequent cause of CHDs arising from a monogenic mutation (Roberts et al., 2007). NS-associated cardiac defects include hypertrophic cardiomyopathy (HCM), PS, and ASD, although CoA, AVC, and mitral valve abnormalities, and VSD can occur. Noonan syndrome with multiple lentigines (NSML) patients present with HCM or PVS, ventricular OFT obstructions, valve abnormalities, ASD, and VSD. CFC patients commonly display PVS, HCM, and ASD, with some instances of CoA, subaortic stenosis and, rarely, arrhythmias. Arrythmias are more common in CS, alongside PS, HCM and, more infrequently, ASD, VSD, and aortic dilation. HCM is also prevalent in patients with neurofibromatosis type 1 syndrome, alongside CoA or PVS.

Zebrafish have been predominantly used to study NS and NSML, although more RASopathy models are being developed (Jindal et al., 2015). NS and NSML models, generated by variant RNA overexpression, recapitulate many features of the human syndrome, but heart defects manifest differently according to the specific mutation. Looping defects are observed upon mutation of *kras* and *ras-like without CAAX 1* (*rit1*), members of the RAS-family of GTPases. The heart tube is enlarged and fails to loop

when *kras* function is lost, while expression of disease-associated mRNA causes a smaller heart with reduced ventricle thickness (Razzaque et al., 2012). *rit1* variants also compromise looping in zebrafish, resulting in hypoplastic chambers, and impaired cardiac function (Aoki, Niihori, Narumi, Kure, & Matsubara, 2008; Koenighofer et al., 2016).

Modeling RASopathy-associated mutations in zebrafish provides insight into mutation-phenotype correlations, especially for different mutations within a single gene. Studies with *protein tyrosine phosphatase, nonreceptor type 11* (*PTPN11*), a gene identified as mutated in patients with either NS or NSML, illustrate this elegantly. Injecting zebrafish embryos with *ptpn11* that contains certain patient-derived mutations induce heart defects, including randomized jogging laterality caused by defects in motile cilia in KV, looping failure, and reduced cardiac function (Bonetti et al., 2014; Jopling, van Geemen, & den Hertog, 2007). However, alternative mutations result in edematous embryos and reduced heart size in adult fish (Miura et al., 2013). This use of zebrafish to discover the phenotypic effects caused by disease-associated alleles clearly indicates that distinct mutations in *ptpn11* have different effects and can cause different diseases.

Studies in zebrafish are useful in informing therapeutic strategies; drugs that have been developed to inhibit Ras signaling in cancer have been effectively used in zebrafish models of CFC and NS (Anastasaki, Estep, Marais, Rauen, & Patton, 2009; Anastasaki, Rauen, & Patton, 2012; Chen et al., 2010; Lee et al., 2014; Wang et al., 2012). Indeed, assaying the strength of the causative mutation can be used to predict the required treatment dose (Jindal et al., 2017). Thus, using zebrafish has advanced both the functional relevance of disease causing mutations and provides a platform for testing therapeutic strategies for treating RASopathy-associated heart disease.

3.6 Williams–Beuren Syndrome

Williams–Beuren syndrome (WBS), also called Williams' syndrome, is a chromosomal microdeletion disorder occurring in 1 in 10,000 individuals (Pober, 2010). WBS is caused by deletion of a critical region (WBSCR), comprising 1.5–1.8 Mb of DNA on chromosome 7 (7q11.23) and containing 26–28 genes (Pober, 2010). Nonallelic homologous recombination between highly homologous blocks of low-copy repeat regions flanking the WBSCR mediates the deletion underlying WBS, resulting in hemizygosity for multiple genes. CHDs are the primary cause of death in WBS patients and 80% of patients have a cardiac abnormality, including VSD, MVP,

and OFT obstruction, but arterial stenosis is most common, including supravalvar aortic stenosis (SVAS), pulmonary arterial stenosis, stenosis of the thoracic aorta, and peripheral pulmonary stenosis (PPS) (Collins, 2013).

Although many genes localize to the WBSCR, *Elastin* (*ELN*) hemizygosity has been demonstrated to contribute to the arteriopathy associated with WBS (Ewart et al., 1993). Elastin is an ECM component that allows the characteristic stretching and recoiling of arteries, and arterial stiffness may be increased in WBS patients as a result of reduced elastin in the ECM (Collins, 2013; Kozel et al., 2014). Indeed, cultured cells isolated from WBS patients show reduced deposition of elastin in the ECM (Urbán et al., 2002). Poor elastin deposition also contributes to increased proliferation of fetal smooth muscle cells, likely causing arterial stenosis in WBS, and may result from altered ECM signaling to cells (Kim, Turnbull, & Guimond, 2011; Moriyama et al., 2016). Collectively, these data suggest that cell fate may be altered by hemizygosity of *ELN* in WBS.

Elastin is critical for the form and function of the BA, the zebrafish OFT, where it is expressed as early as 72 hpf (Miao, Bruce, Bhanji, Davis, & Keeley, 2007). Knockdown of both *elna* and *elnb* reduces BA contraction, although the effect of *elnb* knockdown is more pronounced than that of *elna*, exhibiting additional hypoplasia of the BA (Moriyama et al., 2016). Ectopic cardiomyocytes are observed in the BA of *elna* and *elnb* mutants, but CPC migration patterns are not altered. Rather, *elnb* governs the differentiation of CPCs into smooth muscle cells and its absence allows differentiation into cardiomyocytes instead. Such studies improve our understanding of how individual gene deletions contribute to the overall disease etiology.

3.7 Microdeletion Syndrome 22q11.2

22q11.2 deletion syndrome (22q11.2DS) is the most common microdeletion syndrome in humans. Also known as DiGeorge syndrome or CATCH-22 syndrome (*C*ardiac abnormality, *A*bnormal facies, *T*-cell deficient due to thymic hypoplasia, *C*left palate, *H*ypercalcemia due to hypoparathyroidism resulting from **22**q11 deletion), the prevalence is 1 in 4000 births (Devriendt, Fryns, Mortier, van Thienen, & Keymolen, 1998). Nonallelic homologous recombination occurs between repeat elements, resulting in a highly reproducible series of deletions. Consequently, 90% of patients have a 3 Mb deletion which encompasses 90 genes, many of which remain poorly characterized (Emanuel, 2008). Approximately 80% of patients present with CHDs, primarily conotruncal defects, aortic arch abnormalities, and septal

defects. Considering the phenotypes of 22q11.2DS are believed to arise as a result of gene dosage effects, a major advantage of using zebrafish is the ability to manipulate expression levels using morpholinos and mRNA overexpression.

Of the genes deleted in 22q11.2DS, *TBX1* appears to be most important. Deletion or knockdown of *tbx1* in zebrafish causes cardiac defects: the heart fails to jog or loop, with reduced proliferation in the FHF and decreased cell contribution from the SHF (Piotrowski et al., 2003; Zhang, Gui, Wang, Jiang, & Song, 2010). The reduced incorporation of SHF cells at the arterial pole results in impaired development of the OFT (Hami et al., 2011). TBX1 has a central role in regulating the expression of many genes and altering their expression may contribute to 22q11.2DS. For example, WNT11R has been demonstrated to be downstream of TBX1 in a linear pathway regulating heart development (Choe & Crump, 2014; Choudhry & Trede, 2013), while WNT5A is essential for SHF development (Sinha et al., 2015).

The spectrum of phenotypes observed in patients cannot be fully explained by *TBX1* haploinsufficiency, however. Many proteins deleted in 22q11.2DS are involved in mitochondrial function, potentially implicating mitochondrial dysfunction in disease development. Mitochondrial dysfunction can cause neurodevelopmental and neurodegenerative disease, reminiscent of the neurological symptoms of 22q11.2DS patients. Among the mitochondrial genes deleted, the *SLC25A1* ortholog *slc25a1a* was studied in zebrafish (Catalina-Rodriguez et al., 2012). A dose-dependent relationship was established, where decreasing levels of protein associated with increasing mitochondrial depletion and worsening developmental defects, which included reduced heart size and pericardial edema. Furthermore, the phenotypes induced by knockdown of *slc25a1a* could be suppressed by blocking autophagy, identifying a potential new clinical target (Catalina-Rodriguez et al., 2012). This study underscores the utility of zebrafish in studying the mechanism of disease development and identifying targets that might inform new therapeutic approaches.

4. CONCLUSION

Faithful cardiac development is crucial to the health and survival of vertebrate embryos. While cardiac development is well characterized in zebrafish, several important areas remain poorly understood. The details of tube extension and cardiac looping remain unclear, and the minutiae of ballooning are only recently beginning to emerge. Further quantitative

research into the velocity and routes of migrating cells from the FHF, SHF, and CNC are critical to fully understand zebrafish heart development, as is understanding how their integration into the heart affects morphogenetic events. Only with a comprehensive model we will be able to fully appreciate the perturbations to the system that lead to defects.

While zebrafish hearts are simpler than their human counterparts, significant conservation exists between teleosts and humans, both in the basic cellular changes that effect heart development and in the gene mutations that disrupt this process. Each of the complex developmental syndromes discussed herein can be at least partially recapitulated by mutation, deletion, or knockdown of the same genes in zebrafish. While the links between specific human symptoms and corresponding zebrafish heart phenotypes remain complex, this may be a result of inconsistent scoring of cardiac defects within the zebrafish community. In the future, a standardized description of phenotypes in the zebrafish may prove more informative and allow a better correspondence between zebrafish and mammalian CHD phenotypes. Nevertheless, mutations that generate CHDs in humans consistently disrupt cardiac development in fish, and future work should focus on using gene editing technology to create zebrafish with mutations that are presumed to cause disease in humans.

Perhaps the most exciting aspect of modeling CHD with zebrafish is the potential for personalized medicine. Human mutations are fantastically varied and causative mutations within the same gene can have wildly differing effects. The combination of precise genetic manipulation with the ability to perform effective drug screens makes zebrafish ideal for the identification and development of new therapeutic approaches to treat CHDs. Indeed, such work has already proven informative for RASopathies and 22q11.2DS, and similar screens with new mutations will only improve our knowledge. In the future, it should be possible to identify a human CHD-associated mutation, reproduce the mutation in zebrafish to understand the molecular and cellular causes underlying the accompanying heart defect, and then screen for the most appropriate treatment regimen. Thus, zebrafish will remain at the forefront of cardiac development and CHD research.

ACKNOWLEDGMENTS

D.T.G. is funded by an award from the Founders Affiliate of the American Heart Association (#16POST31390023). R.D.B., V.L.P., and M.G.G. are supported by the National Institutes of Health Grants R01HD048584 and R01GM086537. We thank Kari Lenhart, Jon Rosen, and members of the Burdine lab for comments on the manuscript. We apologize to any colleagues whose work we failed to include or discuss more in depth due to space limitations.

REFERENCES

Abe, Y., Aoki, Y., Kuriyama, S., Kawame, H., Okamoto, N., Kurosawa, K., et al. (2012). Prevalence and clinical features of Costello syndrome and cardio-facio-cutaneous syndrome in Japan: Findings from a nationwide epidemiological survey. *American Journal of Medical Genetics. Part A*, *158A*, 1083–1094.

Ai, D., Liu, W., Ma, L., Dong, F., Lu, M. F., Wang, D., et al. (2006). Pitx2 regulates cardiac left-right asymmetry by patterning second cardiac lineage-derived myocardium. *Developmental Biology*, *296*, 437–449.

Amack, J. D. (2014). Salient features of the ciliated organ of asymmetry. *Bioarchitecture*, *4*, 6–15.

Anastasaki, C., Estep, A. L., Marais, R., Rauen, K. A., & Patton, E. E. (2009). Kinase-activating and kinase-impaired cardio-facio-cutaneous syndrome alleles have activity during zebrafish development and are sensitive to small molecule inhibitors. *Human Molecular Genetics*, *18*, 2543–2554.

Anastasaki, C., Rauen, K. A., & Patton, E. E. (2012). Continual low-level MEK inhibition ameliorates cardio-facio-cutaneous phenotypes in zebrafish. *Disease Models & Mechanisms*, *5*, 546–552.

Aoki, Y., Niihori, T., Narumi, Y., Kure, S., & Matsubara, Y. (2008). The RAS/MAPK syndromes: Novel roles of the RAS pathway in human genetic disorders. *Human Mutation*, *29*, 992–1006.

Arrington, C. B., & Yost, H. J. (2009). Extra-embryonic syndecan 2 regulates organ primordia migration and fibrillogenesis throughout the zebrafish embryo. *Development*, *136*, 3143–3152.

Auman, H. J., Coleman, H., Riley, H. E., Olale, F., Tsai, H. J., & Yelon, D. (2007). Functional modulation of cardiac form through regionally confined cell shape changes. *PLoS Biology*, *5*, e53.

Baker, K., Holtzman, N. G., & Burdine, R. D. (2008). Direct and indirect roles for Nodal signaling in two axis conversions during asymmetric morphogenesis of the zebrafish heart. *Proceedings of the National Academy of Sciences of the United States of America*, *105*, 13924–13929.

Balow, S. A., Pierce, L. X., Zentner, G. E., Conrad, P. A., Davis, S., Sabaawy, H. E., et al. (2013). Knockdown of fbxl10/kdm2bb rescues chd7 morphant phenotype in a zebrafish model of CHARGE syndrome. *Developmental Biology*, *382*, 57–69.

Bartman, T., Walsh, E. C., Wen, K. K., McKane, M., Ren, J., Alexander, J., et al. (2004). Early myocardial function affects endocardial cushion development in zebrafish. *PLoS Biology*, *2*, E129.

Basson, C. T., Cowley, G. S., Solomon, S. D., Weissman, B., Poznanski, A. K., Traill, T. A., et al. (1994). The clinical and genetic spectrum of the Holt-Oram syndrome (heart-hand syndrome). *New England Journal of Medicine*, *330*, 885–891.

Bataille, S., Demoulin, N., Devuyst, O., Audrezet, M. P., Dahan, K., Godin, M., et al. (2011). Association of PKD2 (polycystin 2) mutations with left-right laterality defects. *American Journal of Kidney Diseases: The Official Journal of the National Kidney Foundation*, *58*, 456–460.

Beis, D., Bartman, T., Jin, S. W., Scott, I. C., D'Amico, L. A., Ober, E. A., et al. (2005). Genetic and cellular analyses of zebrafish atrioventricular cushion and valve development. *Development*, *132*, 4193–4204.

Berdougo, E., Coleman, H., Lee, D. H., Stainier, D. Y., & Yelon, D. (2003). Mutation of weak atrium/atrial myosin heavy chain disrupts atrial function and influences ventricular morphogenesis in zebrafish. *Development*, *130*, 6121–6129.

Bisgrove, B. W., Snarr, B. S., Emrazian, A., & Yost, H. J. (2005). Polaris and Polycystin-2 in dorsal forerunner cells and Kupffer's vesicle are required for specification of the zebrafish left-right axis. *Developmental Biology*, *287*, 274–288.

Blake, K. D., & Prasad, C. (2006). CHARGE syndrome. *Orphanet Journal of Rare Diseases*, *1*, 1–8.

Blum, M., Weber, T., Beyer, T., & Vick, P. (2009). Evolution of leftward flow. *Seminars in Cell & Developmental Biology*, *20*, 464–471.

Bonetti, M., Rodriguez-Martinez, V., Paardekooper Overman, J., Overvoorde, J., van Eekelen, M., Jopling, C., et al. (2014). Distinct and overlapping functions of ptpn11 genes in Zebrafish development. *PLoS One*, *9*, e94884.

Bruneau, B. G. (2008). The developmental genetics of congenital heart disease. *Nature*, *451*, 943–948.

Bussmann, J., Bakkers, J., & Schulte-Merker, S. (2007). Early endocardial morphogenesis requires Scl/Tal1. *PLoS Genetics*, *3*, e140.

Cai, C. L., Liang, X., Shi, Y., Chu, P. H., Pfaff, S. L., Chen, J., et al. (2003). Isl1 identifies a cardiac progenitor population that proliferates prior to differentiation and contributes a majority of cells to the heart. *Developmental Cell*, *5*, 877–889.

Catalina-Rodriguez, O., Kolukula, V. K., Tomita, Y., Preet, A., Palmieri, F., Wellstein, A., et al. (2012). The mitochondrial citrate transporter, CIC, is essential for mitochondrial homeostasis. *Oncotarget*, *3*, 1220–1235.

Cavanaugh, A. M., Huang, J., & Chen, J. N. (2015). Two developmentally distinct populations of neural crest cells contribute to the zebrafish heart. *Developmental Biology*, *404*(2), 103–112.

Chen, P. C., Wakimoto, H., Conner, D., Araki, T., Yuan, T., Roberts, A., et al. (2010). Activation of multiple signaling pathways causes developmental defects in mice with a Noonan syndrome-associated Sos1 mutation. *The Journal of Clinical Investigation*, *120*, 4353–4365.

Chi, N. C., Shaw, R. M., De Val, S., Kang, G., Jan, L. Y., Black, B. L., et al. (2008). Foxn4 directly regulates tbx2b expression and atrioventricular canal formation. *Genes & Development*, *22*, 734–739.

Ching, Y. H., Ghosh, T. K., Cross, S. J., Packham, E. A., Honeyman, L., Loughna, S., et al. (2005). Mutation in myosin heavy chain 6 causes atrial septal defect. *Nature Genetics*, *37*, 423–428.

Choe, C. P., & Crump, J. G. (2014). Tbx1 controls the morphogenesis of pharyngeal pouch epithelia through mesodermal Wnt11r and Fgf8a. *Development*, *141*, 3583–3593.

Choudhry, P., & Trede, N. S. (2013). DiGeorge syndrome gene tbx1 functions through wnt11r to regulate heart looping and differentiation. *PLoS One*, *8*, e58145.

Chryssostomidis, G., Kanakis, M., Fotiadou, V., Laskari, C., Kousi, T., Apostolidis, C., et al. (2014). Diversity of congenital cardiac defects and skeletal deformities associated with the Holt–Oram syndrome. *International Journal of Surgery Case Reports*, *5*, 389–392.

Collins, R. T. (2013). Cardiovascular disease in Williams syndrome. *Circulation*, *127*, 2125–2134.

de Campos-Baptista, M. I., Holtzman, N. G., Yelon, D., & Schier, A. F. (2008). Nodal signaling promotes the speed and directional movement of cardiomyocytes in zebrafish. *Developmental Dynamics: An Official Publication of the American Association of Anatomists*, *237*, 3624–3633.

De Domenico, I., Vaughn, M. B., Yoon, D., Kushner, J. P., Ward, D. M., & Kaplan, J. (2007). Zebrafish as a model for defining the functional impact of mammalian ferroportin mutations. *Blood*, *110*, 3780–3783.

de Pater, E., Clijsters, L., Marques, S. R., Lin, Y. F., Garavito-Aguilar, Z. V., Yelon, D., et al. (2009). Distinct phases of cardiomyocyte differentiation regulate growth of the zebrafish heart. *Development*, *136*, 1633–1641.

Deardorff, M. A., Wilde, J. J., Albrecht, M., Dickinson, E., Tennstedt, S., Braunholz, D., et al. (2012). RAD21 mutations cause a human cohesinopathy. *The American Journal of Human Genetics*, *90*, 1014–1027.

Devriendt, K., Fryns, J. P., Mortier, G., van Thienen, M. N., & Keymolen, K. (1998). The annual incidence of DiGeorge/velocardiofacial syndrome. *Journal of Medical Genetics*, *35*, 789–790.

Emanuel, B. S. (2008). Molecular mechanisms and diagnosis of chromosome 22q11.2 rearrangements. *Developmental Disabilities Research Reviews*, *14*, 11–18.

Ewart, A. K., Morris, C. A., Atkinson, D., Jin, W., Sternes, K., Spallone, P., et al. (1993). Hemizygosity at the elastin locus in a developmental disorder, Williams syndrome. *Nature Genetics*, *5*, 11–16.

Fakhro, K. A., Choi, M., Ware, S. M., Belmont, J. W., Towbin, J. A., Lifton, R. P., et al. (2011). Rare copy number variations in congenital heart disease patients identify unique genes in left-right patterning. *Proceedings of the National Academy of Sciences of the United States of America*, *108*, 2915–2920.

Fish, J. E., Wythe, J. D., Xiao, T., Bruneau, B. G., Stainier, D. Y., Srivastava, D., et al. (2011). A Slit/miR-218/Robo regulatory loop is required during heart tube formation in zebrafish. *Development*, *138*, 1409–1419.

Forouhar, A. S., Liebling, M., Hickerson, A., Nasiraei-Moghaddam, A., Tsai, H. J., Hove, J. R., et al. (2006). The embryonic vertebrate heart tube is a dynamic suction pump. *Science*, *312*, 751–753.

Fukushima, N., Ishii, I., Contos, J. J., Weiner, J. A., & Chun, J. (2001). Lysophospholipid receptors. *Annual Review of Pharmacology and Toxicology*, *41*, 507–534.

Gage, P. J., Suh, H., & Camper, S. A. (1999). Dosage requirement of Pitx2 for development of multiple organs. *Development*, *126*, 4643–4651.

Garavito-Aguilar, Z. V., Riley, H. E., & Yelon, D. (2010). Hand2 ensures an appropriate environment for cardiac fusion by limiting Fibronectin function. *Development*, *137*, 3215–3220.

Garrity, D. M., Childs, S., & Fishman, M. C. (2002). The heartstrings mutation in zebrafish causes heart/fin Tbx5 deficiency syndrome. *Development*, *129*, 4635–4645.

Gering, M., Yamada, Y., Rabbitts, T. H., & Patient, R. K. (2003). Lmo2 and Scl/Tal1 convert non-axial mesoderm into haemangioblasts which differentiate into endothelial cells in the absence of Gata1. *Development*, *130*, 6187–6199.

Ghosh, T. K., Song, F. F., Packham, E. A., Buxton, S., Robinson, T. E., Ronksley, J., et al. (2009). Physical interaction between TBX5 and MEF2C is required for early heart development. *Molecular and Cellular Biology*, *29*, 2205–2218.

Granados-Riveron, J. T., Ghosh, T. K., Pope, M., Bu'Lock, F., Thornborough, C., Eason, J., et al. (2010). Alpha-cardiac myosin heavy chain (MYH6) mutations affecting myofibril formation are associated with congenital heart defects. *Human Molecular Genetics*, *19*, 4007–4016.

Grimes, A. C., Stadt, H. A., Shepherd, I. T., & Kirby, M. L. (2006). Solving an enigma: Arterial pole development in the zebrafish heart. *Developmental Biology*, *290*, 265–276.

Guimier, A., Gabriel, G. C., Bajolle, F., Tsang, M., Liu, H., Noll, A., et al. (2015). MMP21 is mutated in human heterotaxy and is required for normal left-right asymmetry in vertebrates. *Nature Genetics*, *47*, 1260–1263.

Guner-Ataman, B., Paffett-Lugassy, N., Adams, M. S., Nevis, K. R., Jahangiri, L., Obregon, P., et al. (2013). Zebrafish second heart field development relies on progenitor specification in anterior lateral plate mesoderm and nkx2.5 function. *Development*, *140*, 1353–1363.

Haffter, P., Granato, M., Brand, M., Mullins, M. C., Hammerschmidt, M., Kane, D. A., et al. (1996). The identification of genes with unique and essential functions in the development of the zebrafish, Danio rerio. *Development*, *123*, 1–36.

Hamada, H., & Tam, P. P. (2014). Mechanisms of left-right asymmetry and patterning: Driver, mediator and responder. *F1000prime reports*, *6*, 110.

Hami, D., Grimes, A. C., Tsai, H. J., & Kirby, M. L. (2011). Zebrafish cardiac development requires a conserved secondary heart field. *Development*, *138*, 2389–2398.

Harvey, R. P., & Rosenthal, N. (1999). *Heart development*. London: Academic Press.

Hatcher, C. J., Goldstein, M. M., Mah, C. S., Delia, C. S., & Basson, C. T. (2000). Identification and localization of TBX5 transcription factor during human cardiac morphogenesis. *Developmental Dynamics: An Official Publication of the American Association of Anatomists*, *219*, 90–95.

Hinits, Y., Pan, L., Walker, C., Dowd, J., Moens, C. B., & Hughes, S. M. (2012). Zebrafish Mef2ca and Mef2cb are essential for both first and second heart field cardiomyocyte differentiation. *Developmental Biology*, *369*, 199–210.

Hisano, Y., Ota, S., Takada, S., & Kawahara, A. (2013). Functional cooperation of spns2 and fibronectin in cardiac and lower jaw development. *Biology Open*, *2*, 789–794.

Holt, M., & Oram, S. (1960). Familial heart disease with skeletal malformations. *British Heart Journal*, *22*, 236–242.

Holtzinger, A., & Evans, T. (2005). Gata4 regulates the formation of multiple organs. *Development*, *132*, 4005–4014.

Holtzinger, A., & Evans, T. (2007). Gata5 and Gata6 are functionally redundant in zebrafish for specification of cardiomyocytes. *Developmental Biology*, *312*, 613–622.

Holtzman, N. G., Schoenebeck, J. J., Tsai, H. J., & Yelon, D. (2007). Endocardium is necessary for cardiomyocyte movement during heart tube assembly. *Development*, *134*, 2379–2386.

Horne-Badovinac, S., Lin, D., Waldron, S., Schwarz, M., Mbamalu, G., Pawson, T., et al. (2001). Positional cloning of heart and soul reveals multiple roles for PKC lambda in zebrafish organogenesis. *Current Biology: CB*, *11*, 1492–1502.

Horsfield, J. A., Print, C. G., & Monnich, M. (2012). Diverse developmental disorders from the one ring: Distinct molecular pathways underlie the cohesinopathies. *Frontiers in Genetics*, *3*, 171.

Icardo, J. M., & Sanchez de Vega, M. J. (1991). Spectrum of heart malformations in mice with situs solitus, situs inversus, and associated visceral heterotaxy. *Circulation*, *84*, 2547–2558.

Ji, Y., Buel, S. M., & Amack, J. D. (2016). Mutations in zebrafish pitx2 model congenital malformations in Axenfeld-Rieger syndrome but do not disrupt left-right placement of visceral organs. *Developmental Biology*, *416*, 69–81.

Jindal, G. A., Goyal, Y., Burdine, R. D., Rauen, K. A., & Shvartsman, S. Y. (2015). RASopathies: Unraveling mechanisms with animal models. *Disease Models & Mechanisms*, *8*, 769–782.

Jindal, G. A., Goyal, Y., Yamaya, K., Futran, A. S., Kountouridis, I., Balgobin, C. A., et al. (2017). In vivo severity ranking of Ras pathway mutations associated with developmental disorders. *Proceedings of the National Academy of Sciences of the United States*. http://dx.doi.org/10.1073/pnas.1615651114, pii:201615651, (Epub ahead of print).

Jopling, C., van Geemen, D., & den Hertog, J. (2007). Shp2 knockdown and Noonan/LEOPARD mutant Shp2-induced gastrulation defects. *PLoS Genetics*, *3*, e225.

Kamura, K., Kobayashi, D., Uehara, Y., Koshida, S., Iijima, N., Kudo, A., et al. (2011). Pkd1l1 complexes with Pkd2 on motile cilia and functions to establish the left-right axis. *Development*, *138*, 1121–1129.

Kawahara, A., Nishi, T., Hisano, Y., Fukui, H., Yamaguchi, A., & Mochizuki, N. (2009). The sphingolipid transporter spns2 functions in migration of zebrafish myocardial precursors. *Science*, *323*, 524–527.

Keegan, B. R., Meyer, D., & Yelon, D. (2004). Organization of cardiac chamber progenitors in the zebrafish blastula. *Development*, *131*, 3081–3091.

Keyte, A., & Hutson, M. R. (2012). The neural crest in cardiac congenital anomalies. *Differentiation; Research in Biological Diversity*, *84*, 25–40.

Kikuchi, K., Holdway, J. E., Major, R. J., Blum, N., Dahn, R. D., Begemann, G., et al. (2011). Retinoic acid production by endocardium and epicardium is an injury response essential for zebrafish heart regeneration. *Developmental Cell*, *20*, 397–404.

Kim, S.-H., Turnbull, J., & Guimond, S. (2011). Extracellular matrix and cell signalling: The dynamic cooperation of integrin, proteoglycan and growth factor receptor. *Journal of Endocrinology*, *209*, 139–151.

Kodo, K., & Yamagishi, H. (2010). GATA transcription factors in congenital heart defects: A commentary on a novel GATA6 mutation in patients with tetralogy of Fallot or atrial septal defect. *Journal of Human Genetics*, *55*, 637–638.

Koenighofer, M., Hung, C. Y., McCauley, J. L., Dallman, J., Back, E. J., Mihalek, I., et al. (2016). Mutations in RIT1 cause Noonan syndrome—Additional functional evidence and expanding the clinical phenotype. *Clinical Genetics*, *89*, 359–366.

Kozel, B. A., Danback, J., Waxler, J., Knutsen, R. H., Fuentes, L. d. l., Reusz, G. S., et al. (2014). Williams syndrome predisposes to vascular stiffness modified by anti-hypertensive use and copy number changes in NCF1. *Hypertension*, *63*, 74–79.

Krantz, I. D., McCallum, J., DeScipio, C., Kaur, M., Gillis, L. A., Yaeger, D., et al. (2004). Cornelia de Lange syndrome is caused by mutations in NIPBL, the human homolog of Drosophila melanogaster Nipped-B. *Nature Genetics*, *36*, 631–635.

Kupperman, E., An, S., Osborne, N., Waldron, S., & Stainier, D. Y. (2000). A sphingosine-1-phosphate receptor regulates cell migration during vertebrate heart development. *Nature*, *406*, 192–195.

LaHaye, S., Lincoln, J., & Garg, V. (2014). Genetics of valvular heart disease. *Current Cardiology Reports*, *16*, 487.

Lalani, S. R., Safiullah, A. M., Molinari, L. M., Fernbach, S. D., Martin, D. M., & Belmont, J. W. (2004). SEMA3E mutation in a patient with CHARGE syndrome. *Journal of Medical Genetics*, *41*, e94.

Lazic, S., & Scott, I. C. (2011). Mef2cb regulates late myocardial cell addition from a second heart field-like population of progenitors in zebrafish. *Developmental Biology*, *354*, 123–133.

Lee, Y. S., Ehninger, D., Zhou, M., Oh, J. Y., Kang, M., Kwak, C., et al. (2014). Mechanism and treatment for learning and memory deficits in mouse models of Noonan syndrome. *Nature Neuroscience*, *17*, 1736–1743.

Lenhart, K. F., Holtzman, N. G., Williams, J. R., & Burdine, R. D. (2013). Integration of nodal and BMP signals in the heart requires FoxH1 to create left-right differences in cell migration rates that direct cardiac asymmetry. *PLoS Genetics*, *9*, e1003109.

Levin, M., Pagan, S., Roberts, D. J., Cooke, J., Kuehn, M. R., & Tabin, C. J. (1997). Left/right patterning signals and the independent regulation of different aspects of situs in the chick embryo. *Developmental Biology*, *189*, 57–67.

Li, Y., Klena, N. T., Gabriel, G. C., Liu, X., Kim, A. J., Lemke, K., et al. (2015). Global genetic analysis in mice unveils central role for cilia in congenital heart disease. *Nature*, *521*, 520–524.

Li, Y. X., Zdanowicz, M., Young, L., Kumiski, D., Leatherbury, L., & Kirby, M. L. (2003). Cardiac neural crest in zebrafish embryos contributes to myocardial cell lineage and early heart function. *Developmental Dynamics: An Official Publication of the American Association of Anatomists*, *226*, 540–550.

Liebling, M., Forouhar, A. S., Wolleschensky, R., Zimmermann, B., Ankerhold, R., Fraser, S. E., et al. (2006). Rapid three-dimensional imaging and analysis of the beating embryonic heart reveals functional changes during development. *Developmental Dynamics: An Official Publication of the American Association of Anatomists*, *235*, 2940–2948.

Lin, C. R., Kioussi, C., O'Connell, S., Briata, P., Szeto, D., Liu, F., et al. (1999). Pitx2 regulates lung asymmetry, cardiac positioning and pituitary and tooth morphogenesis. *Nature*, *401*, 279–282.

Long, S., Ahmad, N., & Rebagliati, M. (2003). The zebrafish nodal-related gene southpaw is required for visceral and diencephalic left-right asymmetry. *Development*, *130*, 2303–2316.

Losada, A. (2014). Cohesin in cancer: Chromosome segregation and beyond. *Nature Reviews. Cancer*, *14*, 389–393.

Lu, M. F., Pressman, C., Dyer, R., Johnson, R. L., & Martin, J. F. (1999). Function of Rieger syndrome gene in left-right asymmetry and craniofacial development. *Nature*, *401*, 276–278.

Maceyka, M., Payne, S. G., Milstien, S., & Spiegel, S. (2002). Sphingosine kinase, sphingosine-1-phosphate, and apoptosis. *Biochimica et Biophysica Acta*, *1585*, 193–201.

Marques, S. R., Lee, Y., Poss, K. D., & Yelon, D. (2008). Reiterative roles for FGF signaling in the establishment of size and proportion of the zebrafish heart. *Developmental Biology*, *321*, 397–406.

McDermott, D. A., Bressan, M. C., He, J., Lee, J. S., Aftimos, S., Brueckner, M., et al. (2005). TBX5 genetic testing validates strict clinical criteria for Holt–Oram syndrome. *Pediatric Research*, *58*, 981–986.

Miao, M., Bruce, A., Bhanji, T., Davis, E., & Keeley, F. (2007). Differential expression of two tropoelastin genes in zebrafish. *Matrix Biology*, *26*, 115–124.

Michaelis, C., Ciosk, R., & Nasmyth, K. (1997). Cohesins: Chromosomal proteins that prevent premature separation of sister chromatids. *Cell*, *91*, 35–45.

Miura, K., Wakayama, Y., Tanino, M., Orba, Y., Sawa, H., Hatakeyama, M., et al. (2013). Involvement of EphA2-mediated tyrosine phosphorylation of Shp2 in Shp2-regulated activation of extracellular signal-regulated kinase. *Oncogene*, *32*, 5292–5301.

Miura, G. I., & Yelon, D. (2011). A guide to analysis of cardiac phenotypes in the zebrafish embryo. *Methods in Cell Biology*, *101*, 161–180.

Moriyama, Y., Ito, F., Takeda, H., Yano, T., Okabe, M., Kuraku, S., et al. (2016). Evolution of the fish heart by sub/neofunctionalization of an elastin gene. *Nature Communications*, 7, 10397.

Mozaffarian, D., Benjamin, E. J., Go, A. S., Arnett, D. K., Blaha, M. J., Cushman, M., et al. (2016). Heart disease and stroke statistics-2016 update: A report from the American Heart Association. *Circulation*, *133*, e38–e360.

Muto, A., Calof, A. L., Lander, A. D., & Schilling, T. F. (2011). Multifactorial origins of heart and gut defects in nipbl-deficient zebrafish, a model of Cornelia de Lange Syndrome. *PLoS Biology*, *9*, e1001181.

Nakhleh, N., Francis, R., Giese, R. A., Tian, X., Li, Y., Zariwala, M. A., et al. (2012). High prevalence of respiratory ciliary dysfunction in congenital heart disease patients with heterotaxy. *Circulation*, *125*, 2232–2242.

Noel, E. S., Verhoeven, M., Lagendijk, A. K., Tessadori, F., Smith, K., Choorapoikayil, S., et al. (2013). A Nodal-independent and tissue-intrinsic mechanism controls heart-looping chirality. *Nature Communications*, *4*, 2754.

Norris, D. P., & Grimes, D. T. (2012). Developmental biology. Cilia discern left from right. *Science*, *338*, 206–207.

Osborne, N., Brand-Arzamendi, K., Ober, E. A., Jin, S. W., Verkade, H., Holtzman, N. G., et al. (2008). The spinster homolog, two of hearts, is required for sphingosine 1-phosphate signaling in zebrafish. *Current Biology: CB*, *18*, 1882–1888.

Padmanabhan, A., Lee, J. S., Ismat, F. A., Lu, M. M., Lawson, N. D., Kanki, J. P., et al. (2009). Cardiac and vascular functions of the zebrafish orthologues of the type I neurofibromatosis gene NFI. *Proceedings of the National Academy of Sciences of the United States of America*, *106*, 22305–22310.

Palencia-Desai, S., Rost, M. S., Schumacher, J. A., Ton, Q. V., Craig, M. P., Baltrunaite, K., et al. (2015). Myocardium and BMP signaling are required for endocardial differentiation. *Development*, *142*, 2304–2315.

Patten, S. A., Jacobs-McDaniels, N. L., Zaouter, C., Drapeau, P., Albertson, R. C., & Moldovan, F. (2012). Role of Chd7 in zebrafish: A model for CHARGE syndrome. *PLoS One*, *7*, e31650.

Peal, D. S., Lynch, S. N., & Milan, D. J. (2011). Patterning and development of the atrioventricular canal in zebrafish. *Journal of Cardiovascular Translational Research*, *4*, 720–726.

Perner, B., Englert, C., & Bollig, F. (2007). The Wilms tumor genes wt1a and wt1b control different steps during formation of the zebrafish pronephros. *Developmental Biology*, *309*, 87–96.

Peterson, R. T., Mably, J. D., Chen, J. N., & Fishman, M. C. (2001). Convergence of distinct pathways to heart patterning revealed by the small molecule concentramide and the mutation heart-and-soul. *Current Biology: CB*, *11*, 1481–1491.

Piotrowski, T., Ahn, D. G., Schilling, T. F., Nair, S., Ruvinsky, I., Geisler, R., et al. (2003). The zebrafish van gogh mutation disrupts tbx1, which is involved in the DiGeorge deletion syndrome in humans. *Development*, *130*, 5043–5052.

Pober, B. R. (2010). Williams–Beuren syndrome. *The New England Journal of Medicine*, *362*, 239–252.

Poon, K.-L., Liebling, M., Kondrychyn, I., Garcia-Lecea, M., & Korzh, V. (2010). Zebrafish cardiac enhancer trap lines: New tools for in vivo studies of cardiovascular development and disease. *Developmental Dynamics*, *239*, 914–926.

Ramsdell, A. F. (2005). Left-right asymmetry and congenital cardiac defects: Getting to the heart of the matter in vertebrate left-right axis determination. *Developmental Biology*, *288*, 1–20.

Rauen, K. A. (2013). The RASopathies. *Annual Review of Genomics and Human Genetics*, *14*, 355–369.

Razzaque, M. A., Komoike, Y., Nishizawa, T., Inai, K., Furutani, M., Higashinakagawa, T., et al. (2012). Characterization of a novel KRAS mutation identified in Noonan syndrome. *American Journal of Medical Genetics. Part A*, *158A*, 524–532.

Reischauer, S., Stone, O. A., Villasenor, A., Chi, N., Jin, S. W., Martin, M., et al. (2016). Cloche is a bHLH-PAS transcription factor that drives haemato-vascular specification. *Nature*, *535*, 294–298.

Richards, A. A., & Garg, V. (2010). Genetics of congenital heart disease. *Current Cardiology Reviews*, *6*, 91–97.

Roberts, A. E., Araki, T., Swanson, K. D., Montgomery, K. T., Schiripo, T. A., Joshi, V. A., et al. (2007). Germline gain-of-function mutations in SOS1 cause Noonan syndrome. *Nature Genetics*, *39*, 70–74.

Rochais, F., Mesbah, K., & Kelly, R. G. (2009). Signaling pathways controlling second heart field development. *Circulation Research*, *104*, 933–942.

Roger, G., Morisseau-Durand, M. P., Van Den Abbeele, T., Nicollas, R., Triglia, J. M., Narcy, P., et al. (1999). The CHARGE association: The role of tracheotomy. *Archives of Otolaryngology—Head & Neck Surgery*, *125*, 33–38.

Rohr, S., Bit-Avragim, N., & Abdelilah-Seyfried, S. (2006). Heart and soul/PRKCi and nagie oko/Mpp5 regulate myocardial coherence and remodeling during cardiac morphogenesis. *Development*, *133*, 107–115.

Rohr, S., Otten, C., & Abdelilah-Seyfried, S. (2008). Asymmetric involution of the myocardial field drives heart tube formation in zebrafish. *Circulation Research*, *102*, e12–e19.

Rose, B. A., Force, T., & Wang, Y. (2010). Mitogen-activated protein kinase signaling in the heart: Angels versus demons in a heart-breaking tale. *Physiological Reviews*, *90*, 1507–1546. http://dx.doi.org/10.1152/physrev.00054.02009.

Rothschild, S. C., Easley, C. A. t., Francescatto, L., Lister, J. A., Garrity, D. M., & Tombes, R. M. (2009). Tbx5-mediated expression of Ca(2+)/calmodulin-dependent

protein kinase II is necessary for zebrafish cardiac and pectoral fin morphogenesis. *Developmental Biology*, *330*, 175–184.

Ryan, A. K., Blumberg, B., Rodriguez-Esteban, C., Yonei-Tamura, S., Tamura, K., Tsukui, T., et al. (1998). Pitx2 determines left-right asymmetry of internal organs in vertebrates. *Nature*, *394*, 545–551.

Sakaguchi, T., Kikuchi, Y., Kuroiwa, A., Takeda, H., & Stainier, D. Y. (2006). The yolk syncytial layer regulates myocardial migration by influencing extracellular matrix assembly in zebrafish. *Development*, *133*, 4063–4072.

Sampath, K., Cheng, A. M., Frisch, A., & Wright, C. V. (1997). Functional differences among Xenopus nodal-related genes in left-right axis determination. *Development*, *124*, 3293–3302.

Sato, M., Tsai, H. J., & Yost, H. J. (2006). Semaphorin3D regulates invasion of cardiac neural crest cells into the primary heart field. *Developmental Biology*, *298*, 12–21.

Sato, M., & Yost, H. J. (2003). Cardiac neural crest contributes to cardiomyogenesis in zebrafish. *Developmental Biology*, *257*, 127–139.

Scherz, P. J., Huisken, J., Sahai-Hernandez, P., & Stainier, D. Y. (2008). High-speed imaging of developing heart valves reveals interplay of morphogenesis and function. *Development*, *135*, 1179–1187.

Schier, A. F., & Shen, M. M. (2000). Nodal signalling in vertebrate development. *Nature*, *403*, 385–389.

Schnetz, M. P., Bartels, C. F., Shastri, K., Balasubramanian, D., Zentner, G. E., Balaji, R., et al. (2009). Genomic distribution of CHD7 on chromatin tracks H3K4 methylation patterns. *Genome Research*, *19*, 590–601.

Schottenfeld, J., Sullivan-Brown, J., & Burdine, R. D. (2007). Zebrafish curly up encodes a Pkd2 ortholog that restricts left-side-specific expression of southpaw. *Development*, *134*, 1605–1615.

Schulz, Y., Wehner, P., Opitz, L., Salinas-Riester, G., Bongers, E. M., van Ravenswaaij-Arts, C. M., et al. (2014). CHD7, the gene mutated in CHARGE syndrome, regulates genes involved in neural crest cell guidance. *Human Genetics*, *133*, 997–1009.

Schuster, K., Leeke, B., Meier, M., Wang, Y., Newman, T., Burgess, S., et al. (2015). A neural crest origin for cohesinopathy heart defects. *Human Molecular Genetics*, *24*, 7005–7016.

Shen, L., Li, X. F., Shen, A. D., Wang, Q., Liu, C. X., Guo, Y. J., et al. (2010). Transcription factor HAND2 mutations in sporadic Chinese patients with congenital heart disease. *Chinese Medical Journal*, *123*, 1623–1627.

Shoji, W., Isogai, S., Sato-Maeda, M., Obinata, M., & Kuwada, J. Y. (2003). Semaphorin3a1 regulates angioblast migration and vascular development in zebrafish embryos. *Development*, *130*, 3227–3236.

Sinha, T., Li, D., Theveniau-Ruissy, M., Hutson, M. R., Kelly, R. G., & Wang, J. (2015). Loss of Wnt5a disrupts second heart field cell deployment and may contribute to OFT malformations in DiGeorge syndrome. *Human Molecular Genetics*, *24*, 1704–1716.

Smith, K. A., Chocron, S., von der Hardt, S., de Pater, E., Soufan, A., Bussmann, J., et al. (2008). Rotation and asymmetric development of the zebrafish heart requires directed migration of cardiac progenitor cells. *Developmental Cell*, *14*, 287–297.

Stainier, D. Y. (2001). Zebrafish genetics and vertebrate heart formation. *Nature Reviews. Genetics*, *2*, 39–48.

Stainier, D. Y., Fouquet, B., Chen, J. N., Warren, K. S., Weinstein, B. M., Meiler, S. E., et al. (1996). Mutations affecting the formation and function of the cardiovascular system in the zebrafish embryo. *Development*, *123*, 285–292.

Stainier, D. Y., Lee, R. K., & Fishman, M. C. (1993). Cardiovascular development in the zebrafish. I. Myocardial fate map and heart tube formation. *Development*, *119*, 31–40.

Stainier, D. Y., Weinstein, B. M., Detrich, H. W., 3rd, Zon, L. I., & Fishman, M. C. (1995). Cloche, an early acting zebrafish gene, is required by both the endothelial and hematopoietic lineages. *Development*, *121*, 3141–3150.

Staudt, D., & Stainier, D. (2012). Uncovering the molecular and cellular mechanisms of heart development using the zebrafish. *Annual Review of Genetics*, *46*, 397–418.

Sun, X., Zhang, R., Lin, X., & Xu, X. (2008). Wnt3a regulates the development of cardiac neural crest cells by modulating expression of cysteine-rich intestinal protein 2 in rhombomere 6. *Circulation Research*, *102*, 831–839.

Sutherland, M. J., & Ware, S. M. (2009). Disorders of left-right asymmetry: Heterotaxy and situs inversus. *American Journal of Medical Genetics. Part C, Seminars in Medical Genetics*, *151c*, 307–317.

Swaminathan, P. D., Purohit, A., Hund, T. J., & Anderson, M. E. (2012). Calmodulin-dependent protein kinase II: Linking heart failure and arrhythmias. *Circulation Research*, *110*, 1661–1677.

Szeto, D. P., Griffin, K. J. P., & Kimelman, D. (2002). hrT is required for cardiovascular development in zebrafish. *Development*, *129*, 5093–5101.

Targoff, K. L., Schell, T., & Yelon, D. (2008). Nkx genes regulate heart tube extension and exert differential effects on ventricular and atrial cell number. *Developmental Biology*, *322*, 314–321.

Tidyman, W. E., & Rauen, K. A. (2009). The RASopathies: Developmental syndromes of Ras/MAPK pathway dysregulation. *Current Opinion in Genetics & Development*, *19*, 230–236.

Tonkin, E. T., Smith, M., Eichhorn, P., Jones, S., Imamwerdi, B., Lindsay, S., et al. (2004). A giant novel gene undergoing extensive alternative splicing is severed by a Cornelia de Lange-associated translocation breakpoint at 3q26.3. *Human Genetics*, *115*, 139–148.

Totong, R., Schell, T., Lescroart, F., Ryckebusch, L., Lin, Y. F., Zygmunt, T., et al. (2011). The novel transmembrane protein Tmem2 is essential for coordination of myocardial and endocardial morphogenesis. *Development*, *138*, 4199–4205.

Trinh, L. A., & Stainier, D. Y. (2004). Fibronectin regulates epithelial organization during myocardial migration in zebrafish. *Developmental Cell*, *6*, 371–382.

Urbán, Z., Riazi, S., Seidl, T. L., Katahira, J., Smoot, L. B., Chitayat, D., et al. (2002). Connection between elastin haploinsufficiency and increased cell proliferation in patients with supravalvular aortic stenosis and Williams–Beuren syndrome. *The American Journal of Human Genetics*, *71*, 30–44.

Veerkamp, J., Rudolph, F., Cseresnyes, Z., Priller, F., Otten, C., Renz, M., et al. (2013). Unilateral dampening of Bmp activity by nodal generates cardiac left-right asymmetry. *Developmental Cell*, *24*, 660–667.

Vermot, J., Forouhar, A. S., Liebling, M., Wu, D., Plummer, D., Gharib, M., et al. (2009). Reversing blood flows act through klf2a to ensure normal valvulogenesis in the developing heart. *PLoS Biology*, 7, e1000246.

Vetrini, F., D'Alessandro, L. C., Akdemir, Z. C., Braxton, A., Azamian, M. S., Eldomery, M. K., et al. (2016). Bi-allelic mutations in PKD1L1 are associated with laterality defects in humans. *The American Journal of Human Genetics*, *99*, 886–893.

Vissers, L. E. L. M., van Ravenswaaij, C. M. A., Admiraal, R., Hurst, J. A., de Vries, B. B. A., Janssen, I. M., et al. (2004). Mutations in a new member of the chromodomain gene family cause CHARGE syndrome. *Nature Genetics*, *36*, 955–957.

Wang, Y., Kim, E., Wang, X., Novitch, B. G., Yoshikawa, K., Chang, L. S., et al. (2012). ERK inhibition rescues defects in fate specification of Nf1-deficient neural progenitors and brain abnormalities. *Cell*, *150*, 816–830.

Watrin, E., Kaiser, F. J., & Wendt, K. S. (2016). Gene regulation and chromatin organization: Relevance of cohesin mutations to human disease. *Current Opinion in Genetics & Development*, *37*, 59–66.

Wyse, R. K., al-Mahdawi, S., Burn, J., & Blake, K. (1993). Congenital heart disease in CHARGE association. *Pediatric Cardiology*, *14*, 75–81.

Yashiro, K., Shiratori, H., & Hamada, H. (2007). Haemodynamics determined by a genetic programme govern asymmetric development of the aortic arch. *Nature*, *450*, 285–288.

Yelon, D., Horne, S. A., & Stainier, D. Y. (1999). Restricted expression of cardiac myosin genes reveals regulated aspects of heart tube assembly in zebrafish. *Developmental Biology*, *214*, 23–37.

Yelon, D., Ticho, B., Halpern, M. E., Ruvinsky, I., Ho, R. K., Silver, L. M., et al. (2000). The bHLH transcription factor hand2 plays parallel roles in zebrafish heart and pectoral fin development. *Development*, *127*, 2573–2582.

Yoshiba, S., & Hamada, H. (2014). Roles of cilia, fluid flow, and Ca2+ signaling in breaking of left-right symmetry. *Trends in Genetics*, *30*, 10–17.

Zariwala, M. A., Omran, H., & Ferkol, T. W. (2011). The emerging genetics of primary ciliary dyskinesia. *Proceedings of the American Thoracic Society*, *8*, 430–433.

Zentner, G. E., Layman, W. S., Martin, D. M., & Scacheri, P. C. (2010). Molecular and phenotypic aspects of CHD7 mutation in CHARGE syndrome. *American Journal of Medical Genetics. Part A*, *152A*, 674–686.

Zhang, L. F., Gui, Y. H., Wang, Y. X., Jiang, Q., & Song, H. Y. (2010). Effect of Tbx1 knock-down on cardiac performance in zebrafish. *Chinese Medical Journal*, *123*, 1182–1189.

Zhou, Y., Cashman, T. J., Nevis, K. R., Obregon, P., Carney, S. A., Liu, Y., et al. (2011). Latent TGF-beta binding protein 3 identifies a second heart field in zebrafish. *Nature*, *474*, 645–648.